ANNEALING OF COLD-ROLLED AND COATED 300-GRADE SILICON-STEEL AND ITS EFFECT ON PROPERTIES

A Thesis Submitted
in Partial Fulfilment of the Requirements
for the Degree of
MASTER OF TECHNOLOGY

By

P. K. KAR

to the

DEPARTMENT OF METALLURGICAL ENGINEERING
INDIAN INSTITUTE OF TECHNOLOGY, KANPUR

OCTOBER, 1980

24.10.80

CERTIFICATE

This is to certify that this work on 'Annealing of Cold-Rolled and Coated 300-grade Silicon-Steel and its Effect on Properties' has been carried out under my supervision and it has not been submitted elsewhere for a degree.

(G.S. Upadhyaya) 24/10/80
Professor
Department of Metallurgical Engineering
Indian Institute of Technology, Kanpur.

3.11.80

ACKNOWLEDGEMENT

I gratefully thank Dr. G.S. Upadhyaya for his valuable guidance throughout this present investigation.

I sincerely thank the General Manager (Operations), Tata Iron and Steel Co. Ltd., Jamshedpur, for the materials that were provided and for the permission to conduct some of the tests at TISCO. I sincerely thank Dr. T. Mukherjee, DMSS, TISCO, for all the assistance he provided.

I thank all my colleagues for the help and encouragement they provided for completion of this work. Special mention is made about Edwin, Gango, Hamiuddin and Balram.

ABSTRACT

There are two ways by which the electrical and magnetic properties of silicon-steel sheets can be improved. These are either by change of the steel composition during steel making or by the change in grain size and by decreasing the various impurity levels, through various finishing treatments. The present investigation has been aimed at an improvement in the properties of the 300-grade silicon steel sheets entirely through the finishing treatments. Various cold reductions followed by annealing and the use of chemically active coatings which might affect decarburization and desulphurization during subsequent annealing of the sheets have been investigated. There exists a critical level of cold-reduction of 10 pct. and an optimum annealing temperature of 800°C for which the average grain size is maximum and the corresponding core loss values were minimum. In case of the coated samples, some of the coatings give better electrical and magnetic properties after annealing which is explained as due to better decarburization and desulphurization of the steel sheets.

CONTENTS

CHAPTER I

LITERATURE REVIEW

I.1 Introduction

In recent years considerable research has been done in the development of electrical grade steels. This is mainly due to the fact that better performance of electrical equipments and machinery demands superior grade materials. Increasing stringent requirements of electrical grade steels for better service performance has made steel makers seek constant improvements in production technology[1].

Besides controlling the chemical composition and improving deoxidation practice in steel making stage, rolling parameters and subsequent annealing cycles have been precisely determined[2]. Different techniques such as recrystallization and grain growth, decarburisation annealing and annealing in magnetic field have been successfully tried.

Progress during the last decade has been remarkable in the development of electrical grade steels. In the case of non-oriented grade, semiorganic coatings have been developed to improve the electrical properties. Use of these coatings has further helped to improve producitivity by

improving the workability of the sheets. Among the grain oriented electrical steels, the development of grades with increased permeability is reported. With these steels, remarkably reduced hysteresis loss is attained by a high degree of grain-orientation. Decrease in eddy current loss is achieved by the use of certain chemical coatings which induce tensile stresses on the surface. Equipments made from such steels have demonstrated their superiority over conventional counterparts in their lower total loss, lower exciting current and lower noise.

Although, considerable effort has been put in the development of transformer grade electricals steels, very little work has been reported on the development of dynamo grade electrical sheet steels.

I.2 Factors Affecting Electrical and Magnetic Properties

The magnetic properties of steel depends on chemical composition and microstructure. Certain properties like saturation induction B_s, Intensity of magnetisation I_s, the magnetostriction λ, the curie temperature θ, and crystal anisotropy constant K, based almost entirely on the chemistry are referred to as structure insensitive properties. The structure sensitive properties are permeability μ, coercive force H_c. The size of the hysteresis loop, on the otherhand

is greatly influenced by thermal and mechanical treatments which alter the structure of the material[3]. Table 1.1 lists out the structure sensitive and insensitive properties and some of the factors affecting them[4].

Table 1.1 Properties commonly sensitive or insensitive to small changes in structure and some of the factors which effect such changes.

Structure in-sensitive Properties	Structure sensitive Properties	Factors affecting the properties
I_s, saturation Magnetisation	μ, permeability	Composition (gross)
θ, Curie temperature	H_c, coercive force	Impurities
λ_s, Magnetostriction at saturation	W_h, Hysteresis loss	Strain Temperature
K, crystal anisotropy constant		Crystal structure crystal orientation

The structure sensitive properties are of special interest since they determine the ease of magnetisation and the hysteresis loss. Keeping the chemistry of the steel unchanged it is possible to alter the, structure, so as to improve the electromagnetic properties of steel. Eddy-current loss is affected both by the structure-sensitive and structure in-sensitive properties.

I.2.1 Effect of Nominal Chemical Composition:

(i) Effect of Silicon:

The addition of silicon to steel changes magnetic properties like saturation induction B_s, coercive force H_c, maximum permeability μ_{max}, curie point θ, electrical resistivity ρ, Hysteresis loss W_h, and the total specific loss W_T. The saturation-induction[5], Curie point (Fig. 1.1) Total specific loss, hysteresis loss, and the coercive force decrease with the increase in silicon content (Fig. 1.2)[4], whereas properties like maximum permeability, electrical resistivity increase with the increase in silicon content[5].

The phase diagram of Iron-rich iron-silicon alloy is shown in (Fig. 1.3)[4]. The solubility of carbon at room temperature is not greatly influenced by silicon, but the presence of silicon causes the carbon to precipitate largely as graphite rather than as cementite. This has a relatively small effect on the magnetic properties.

(ii) Effect of Carbon:

Effect of small carbon contents on the α, γ boundaries of the iron-silicon equilibrium diagram is shown in (Fig. 1.4)[4]. The gamma-phase characteristic of pure iron,

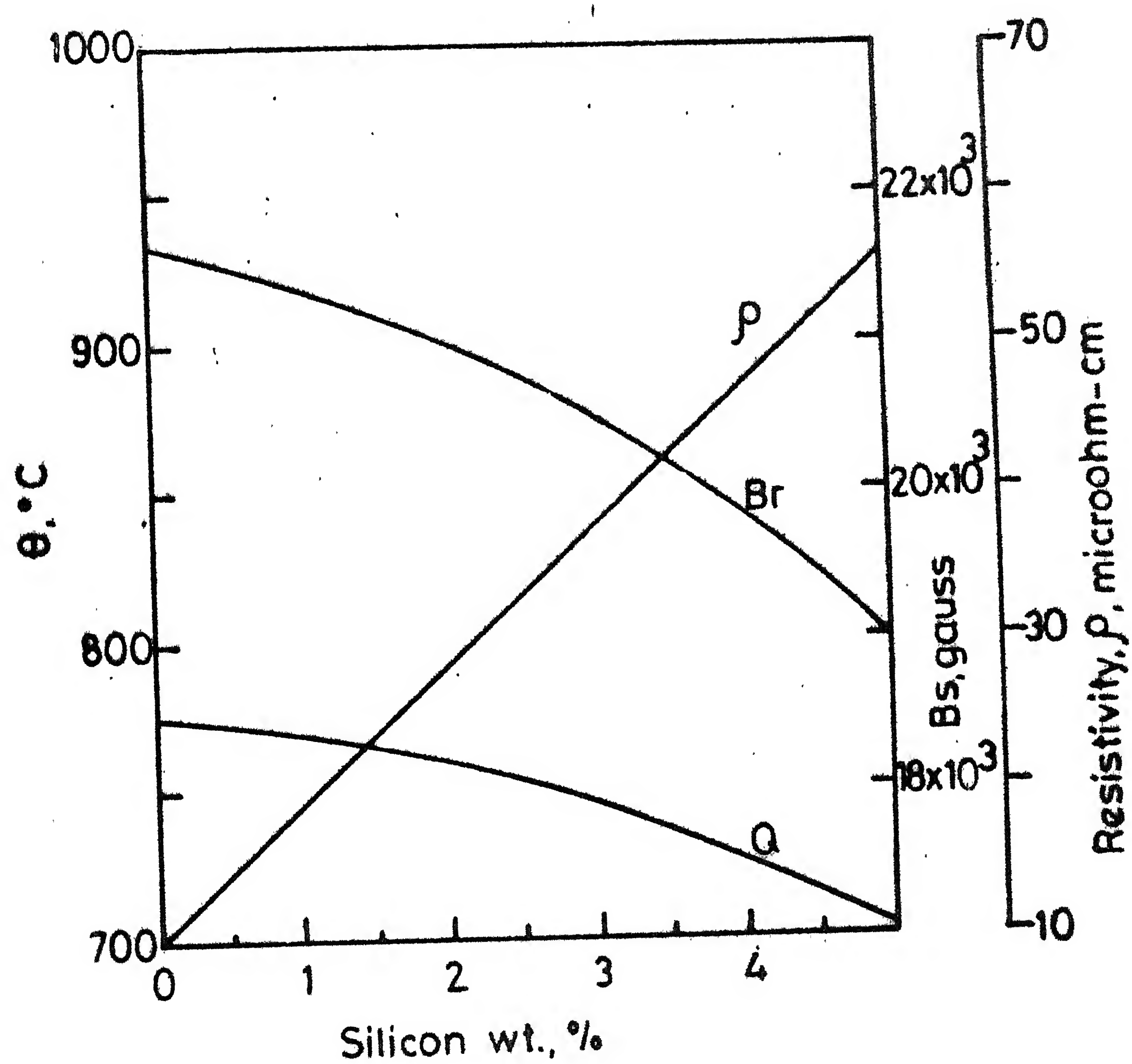

Fig. 1·1 - Effect of silicon content on the electric and magnetic properties of silicon steel.

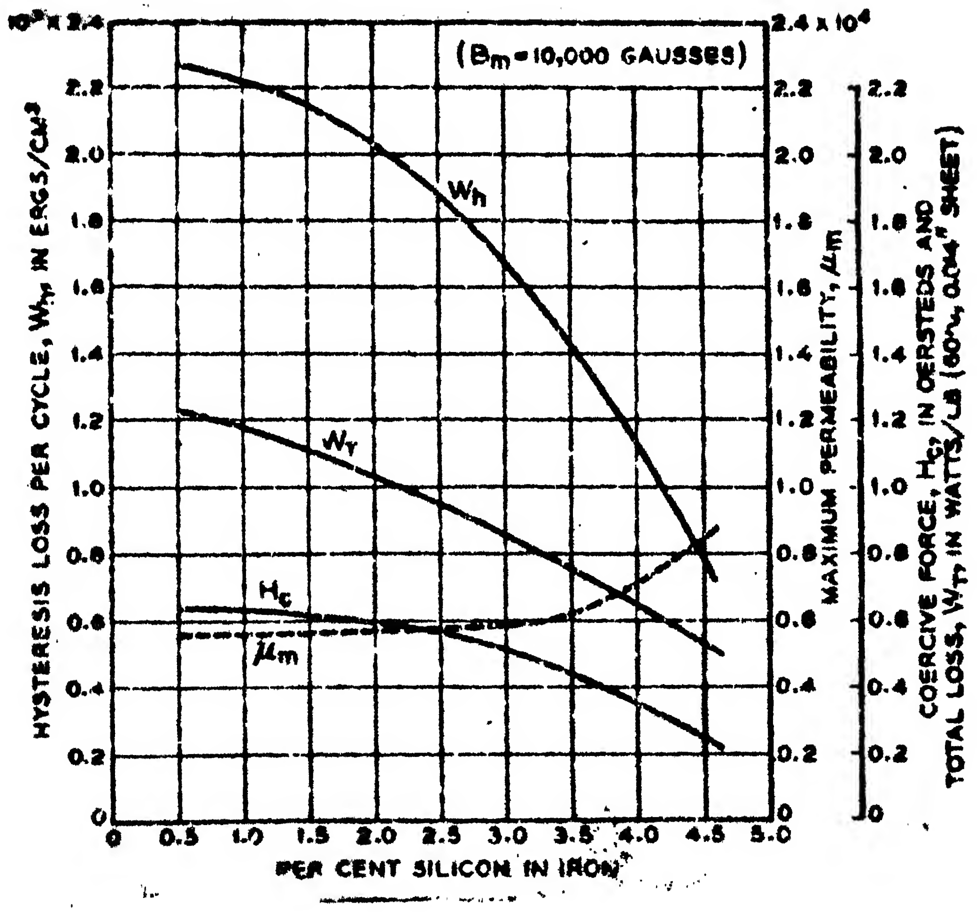

Fig. 1.2. Some magnetic properties of hot-rolled commercial silicon-iron sheet[4].

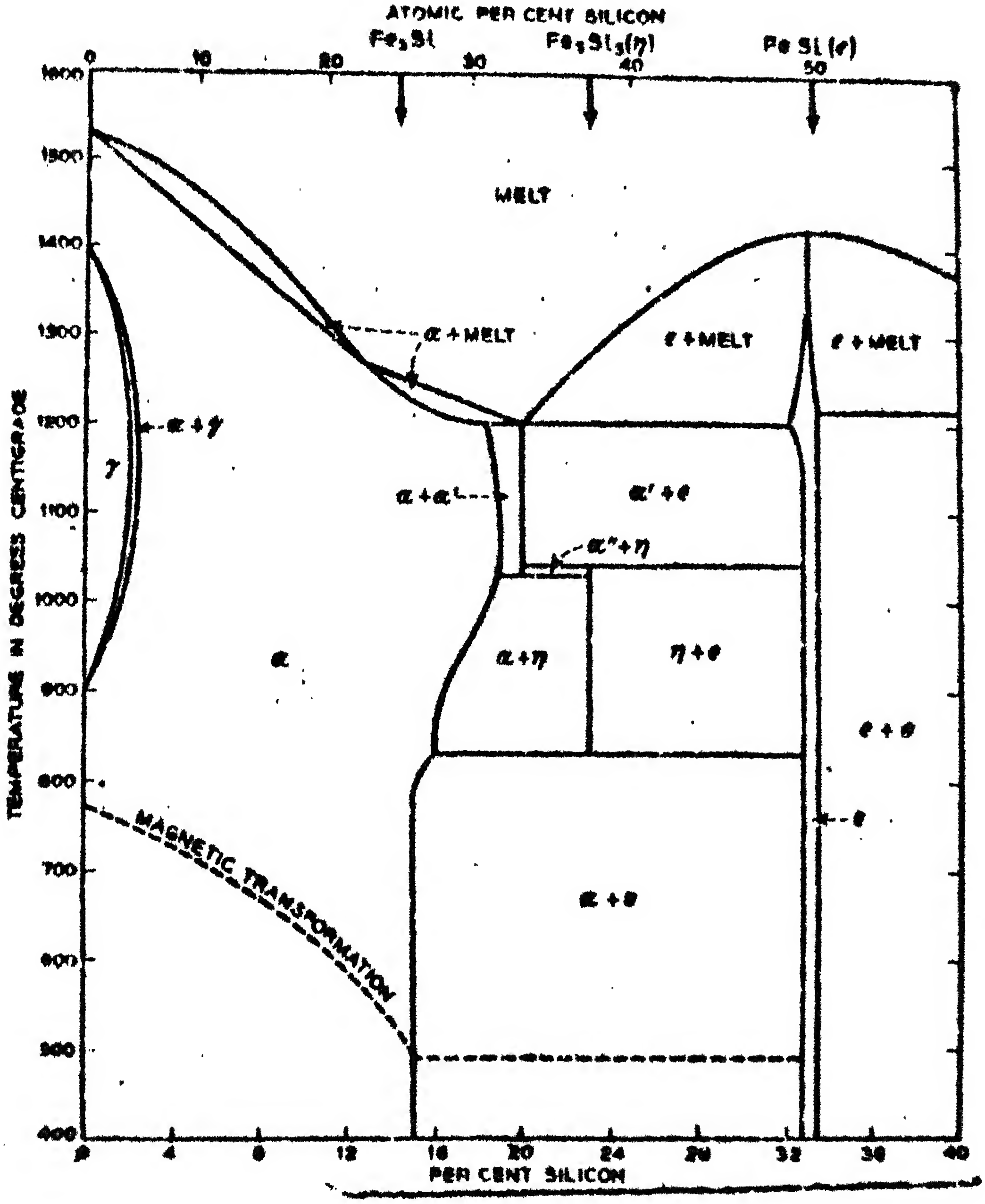

Fig. 1.3. Phase diagram of iron-rich iron-silicon alloys[4].

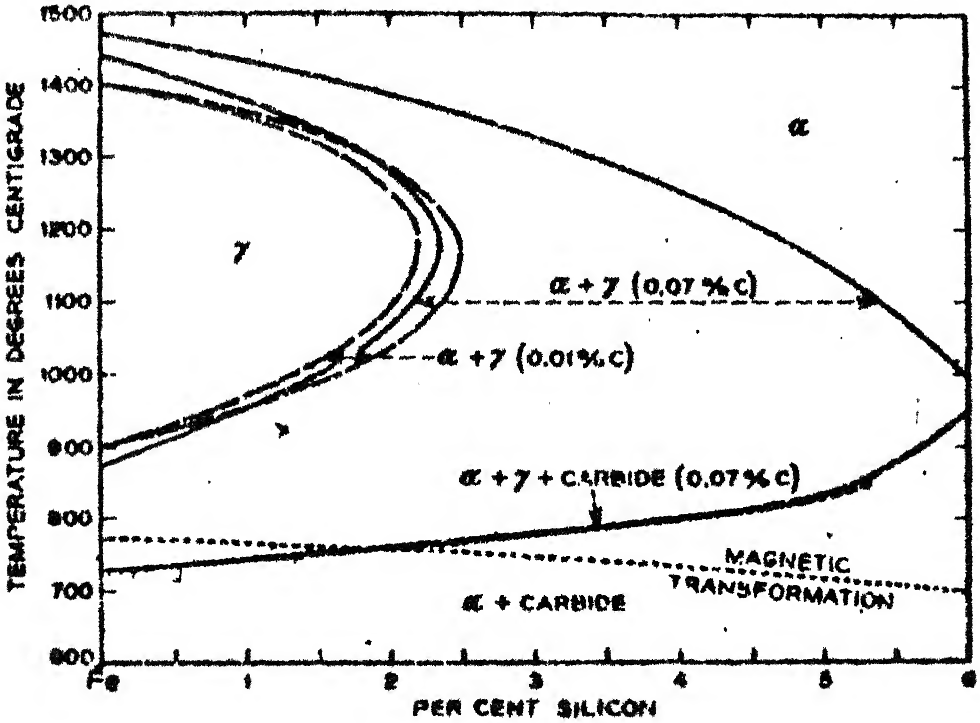

Fig. 1.4. Effect of small carbon contents on the α, γ boundaries of the iron-silicon diagram[4].

does not exist in alloys containing more than 2.5 pct. silicon. But even a small amount of carbon windens the $\alpha + \gamma$ region and extends the boundary between $\alpha + \gamma$ and α beyond 5 pct. silicon content. Therefore, in most commercial alloys, which contain 5 pct. or less silicon, a certain small fraction of material transforms to the γ phase above about 800°C. For this reason conventional annealing is carried out just below this temperature.

The effect of carbon on the magnetic properties of transformer steel have been studied in great detail by many researchers[6]. Core-loss of a transformer steel increases up to a carbon level of 0.015-0.018 pct. due to cementite inclusions present in the structure. With further increase of carbon (above 0.028 pct. carbon), graphitization occurs which results in a decrease in core-loss.

The effect of carbon on hysteresis loss has been reported by several authors[7]. The fact that carbon can exist in steel in different forms makes it necessary to take this into account i.e., whether it occurs in solution, as free carbide, as pearlite or as graphite. Disregarding grain structure, the loss due to presence of carbon is normally represented as

$$Wh = KC$$

where Wh = Hysteresis loss, ergs cm^3 cycle^{-1}

C = Carbon content in steel, pct. and

K = is a constant.

K varies between 2250 and 220,000 depending on carbon level. Thus carbon is byfar the most important impurity affecting magnetic characteristics[2].

The effect of higher carbon on the hysteresis loss and on the minimum reluctivity of iron-silicon alloys is given in Figs. 1.5 and 1.6[5] respectively.

(iii) Effect of Other Impurities:

The presence of impurities[8,9], either in solution or as inclusions disrupts the regularity and continuity of the crystalline arrangement, and this makes domain movements and alignments difficult. Hence an attempt is made to reduce the impurity level to the lowest value in the process of steel making.

The effect of sulphur on hysteresis-loss according to Yensen[10] is normally represented as:

$$Wh = 18,000S$$

where S = pct. sulphur content in steel

Although the effect of oxygen[11,12], on hysteresis loss is normally, not represented in the form of equation,

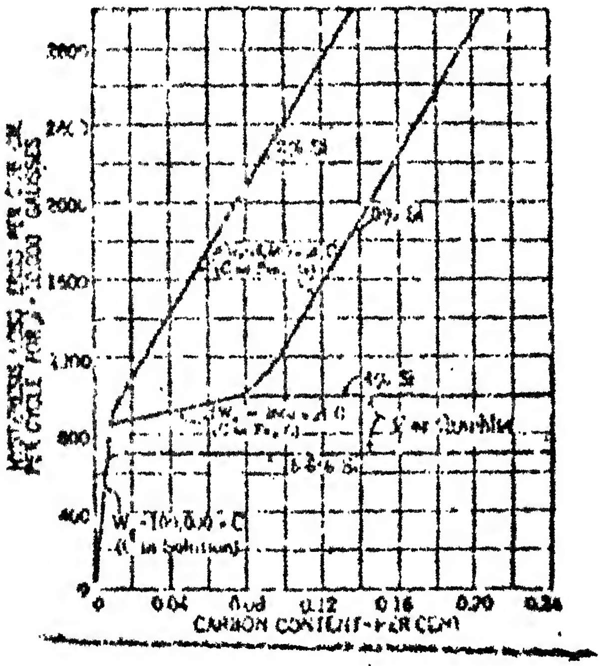

Fig. 1.5. Effect of carbon on the hysteresis loss of iron-silicon alloys[5].
(All other impurities and effect of grain size eliminated)

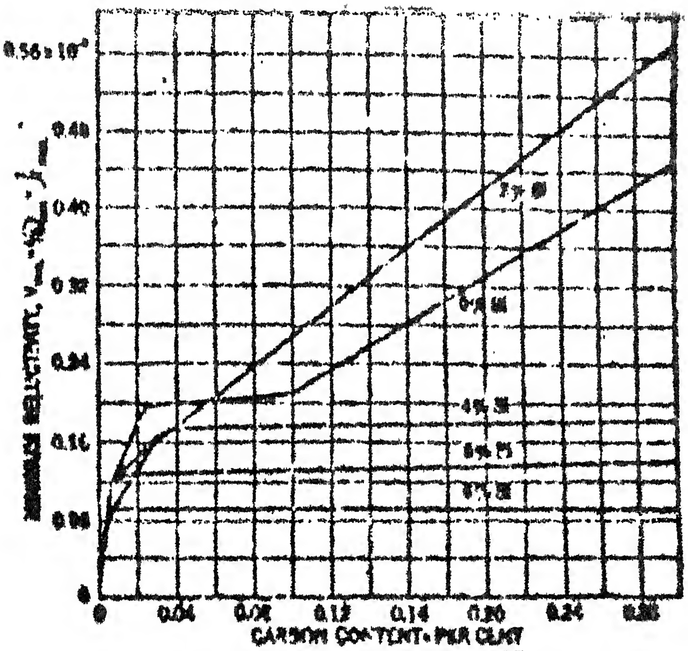

Fig. 1.6. Effect of carbon on minimum reluctivity (reciprocal of maximum permeability) of iron-silicon alloys[5].

(No correction made for incidental impurities or grain size)

the best results are obtained when the difference between pct. of carbon and pct. of oxygen in steel is zero.

The lower loss obtained by balancing the effects of impurities, carbon and oxygen is shown in Fig. 1.7.

The influence of other elements, on magnetic characteristics is generally given by the following equation[7,13]:

$$Wh = 3N + 80C + 16,500\ (C-0.008)$$
$$+ 1800\,S + 1000\,Mn + 13000\,P.$$

Where, N, C, S, Mn, P represent pct. nitrogen, pct. carbon, pct. sulphur, pct. manganese and pct. phosphorous respectively in steel.

I.2.2 Effect of Annealing Treatment

The total electrical losses (coreloss) in a steel can be broken down mainly into hysteresis-loss and eddy-current loss. Those are controlled by the following factors[1].

Hysteresis-loss:
- Grain orientation
- Purity (inclusions, precipitates)
- Internal stress

Eddy-current loss:
- Electrical resistivity (Silicon content)
- Residual tensile stresses (surface coating)
- Size of magnetic domain (grain size)

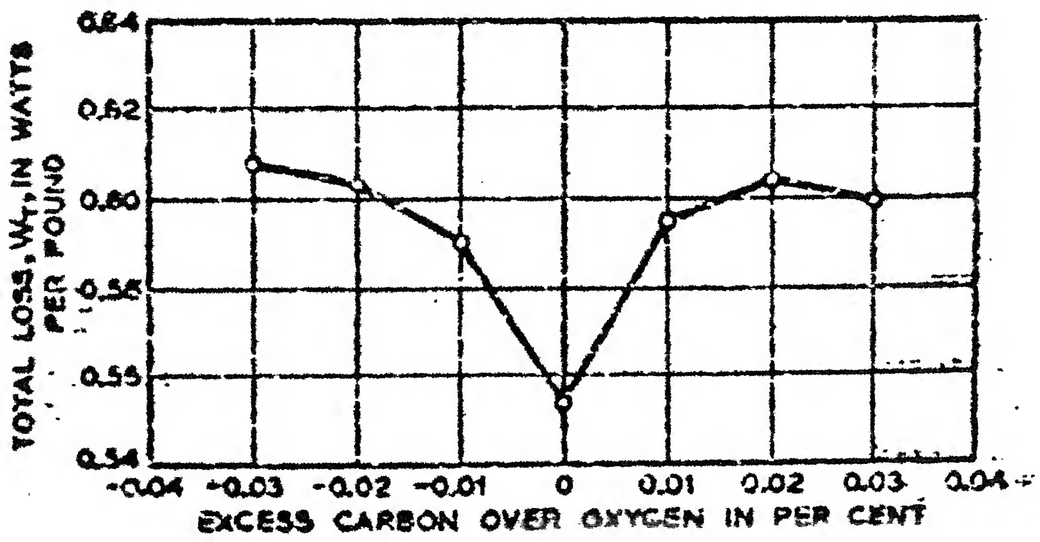

Fig. 1.7. Low-loss caused by balancing of impurities of carbon and oxygen[4].

Purity and electrical resistivity are controlled by the chemical composition and the steel making process adopted. Heat treatment process also determines the magnitude of the above mentioned contributory factors, which increase the electrical losses.

(i) <u>Annealing Temperature</u>:

Generally, higher the annealing temperature, lower is the total core-loss for a hot rolled electrical steel. But, the highest possible annealing temperature which can be used is limited by the chemical composition[4]. From the [Fe-Si] equilibrium diagram (Fig. 1.5), the maximum annealing temperature can be determined. For annealing a low silicon steel (with about 1 pct. Si), a temperature below 900°C is recommended. For steel with higher silicon content (i.e. more than 2 pct. silicon), an annealing temperature above 1000°C is advisable[14].

(ii) <u>Annealing Cycle</u>:

The rate of heating to reach the annealing temperature has a determining influence on final electrical properties of the steel. Good magnetic properties are not obtained if the steel is heated rapidly to the high annealing temperature. For example, when a steel sample is placed in a furnace at

high temperatures, fine grains without texture are formed and the sample has poor magnetic properties[14]. When a sample is gradually heated to the annealing temperature, large grains are formed. Also when annealing is done at relatively lower temperatures, quicker rate of heating is found to be beneficial[15]. To produce a steel with given grain size and with a desired grain orientation, it is necessary to limit the rate of heating for high temperature annealing to 30° C/hr[16].

Cooling of the sheets subsequent to annealing should be done at a rate slow enough not to induce any residual thermal stress.

(iii) Annealing Atmosphere:

Annealing is carried out in a protective atmosphere to avoid oxidation of the surface. The annealing atmosphere generally employed in a sheet mill is cracked ammonia or cracked coke oven gas which is weakly reducing. It contains about 10 pct. H_2, very little oxygen and mostly nitrogen. The effect of other annealing atmospheres such as hydrogen, nitrogen and vacuum have been discussed in literature[12]. Table I.2 gives the effect of annealing atmosphere on carbon content[17].

Table I.2. <u>Effect of Annealing Atmosphere on Carbon content in different Si-Steel grades</u>

Grade of Steel	Treatment	pct. C (wt.)
Non-silicon	As-sheared	0.08
	Nitrogen annealed	0.06
	Decarburization Annealed	0.02
Cr-300	As-sheared	0.03
	Nitrogen annealed	0.03
	De-carburization annealed	0.02
Cr-360	As-sheared	0.05
	Nitrogen annealed	0.03
	Decarburization Annealed	0.02

I.2.3 <u>Effect of Grainsize and Grain-orientation</u>

The effect of grain size and orientation on the properties of electrical steel has been studied extensively. Coercive force and hysteresis losses decrease with increasing grain size. As the grain size increases in the textured steel, hysteresis loss decreases while the magnetic permeabil and magnetic-induction increases[15].

(i) Effect of Grain Size:

The fact that grainsize has an important effect on the magnetic properties of electrical grade sheets, has long since been known[10,18]. The effect of grain size for a given carbon content can be expressed as[2]

$$Wh = 100 \sqrt{\text{ASTM Grain size}}$$

where Wh = hysteresis loss

The degree of preferred orientation and magnetic inductance increase with the coarsening of the grains. A considerable deterioration both of the magnetic induction and of the specific losses is observed when the grains are smaller. Better steel structure is obtained during grain growth and the texture of the finished sheet is more perfect the coarser its grain[16].

In a coarse grained steel, hysteresis loss decreases due to decrease of coercive force and also due to a more favourable texture, although the eddy current loss increases. There is therefore an optimum grain size[19] for which eddy current loss in electrical steels would be minimum.

(ii) Effect of Grain Orientation:

A rapid progress has been brought about by the development of grain oriented steel. This has been achieved by

reducing the hysteresis loss on the following principle. Iron is easily magnetised in certain crystallographic directions. For example it is found that along [001] direction the magnetization is easiest, while it is most difficult to magnetise along [111] direction. [011] is found to be intermediate. It has been discovered that by controlling the rolling process, it is possible to have the (110)[001] texture developed in silicon steels. The grain oriented electrical steel is an aggregate of grains of (110)[001] orientation. Greater the degree of grain orientation, i.e., more grains assume an orientation close to the ideal (110)[001], the better is the magnetic property[1]. Fig. 1.8 shows the effect of grain direction on shape of hysteresis loop for a medium silicon steel. On an average the losses at right angles to the grain are about 14 pct. higher than that for the parallel direction. The losses at an angle of 45° with the direction of rolling are about 6 pct. higher than for parallel-grain samples. The permeability of the perpendicular grain material is about 75 pct. of that of the parallel grain steel for all inductions.

I.2.4 Effect of Mechanical stresses:

Electrical grade sheet is subjected to a variety of strains both elastic and plastic. In general, these strains

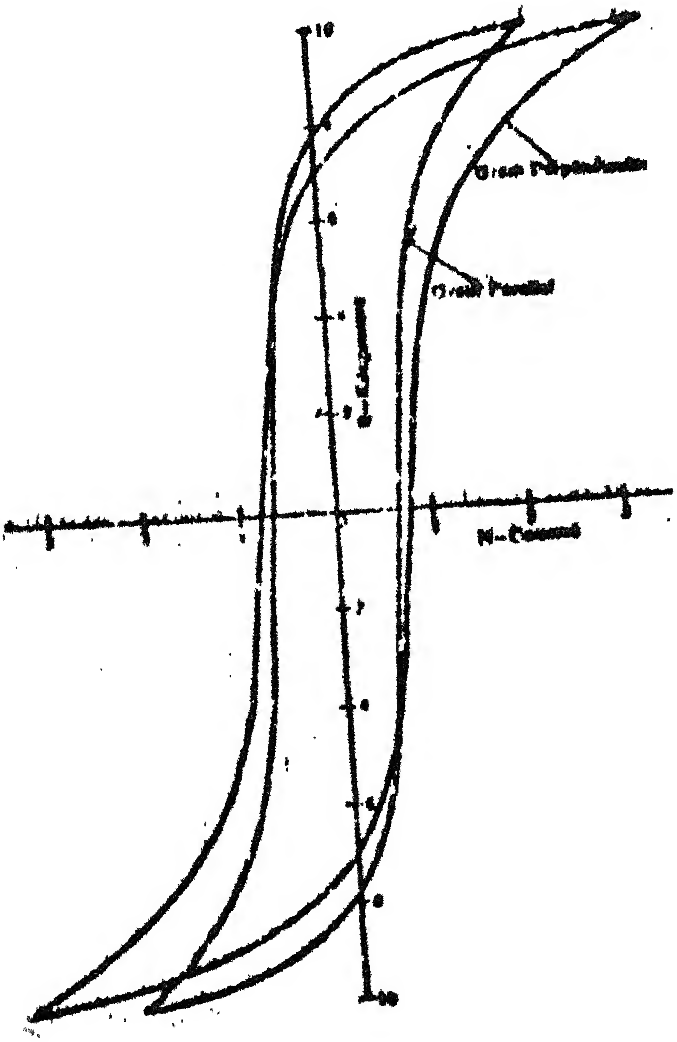

Fig. 1.8. Effect of grein direction on shape of hysteresis loop[5].

have a deleterious effect on magnetic properties. Improper annealing can result in a bent or wavy sheet which when assembled as a laminated magnetic core can get straightened out producing both elastic and plastic strains. Since there is a bending effect, the strains are both compressive and tensile in nature. In the process of punching, the edges of the sheets are strained beyond the elastic limit, producing permanent strains. During annealing process these mechanical strains are relieved. A temperature of 450°C is sufficient to release the punching strains only partially, but a temperature of 750°C not only eliminates them entirely but results in a material superior to the unpunched sheet[5].

I.2.5 Effect of Aging:

In electrical grade steels, both silicon and non-silicon bearing types, a slow deterioration often takes place in the magnetic properties like core loss, permeability and coercive force after the material has been annealed. At room temperature it may take from a few months to a few years for the changes to become perceptible and significant. At a slightly elevated temperature, however, the rate of deterioration can become a cause of concern. This phenomenon is known as magnetic aging.

magnetic aging is considered to be caused primarily by carbon and, or nitrogen, when present in the steel in amounts exceeding their solid solubility limits at room-temperature. In the manufacture of electrical grade steels, the rate of cooling after annealing is not sufficiently slow enough for the excess impurity (C and N) atoms to precipitate during the cooling process. As a result, they precipitate out as a fine dispersoid of carbides and nitrides later when the material is put into service[4]. These precipitates interfere with the motion of domain walls resulting in the phenomenon of magnetic aging.

I.3 Recrystallization and Grain-growth in Silicon Steels

It has been established[20] that by making proper advantage of phenomenon of recrystallization, it is possible to produce electricl grade steel sheets with increased grain-size. The fact that, with increasing grain-size, the core-loss value falls off considerably has long since been established. Thus a very important improvement in the electric grade steel sheets is possible.

It has been reported by several authors[21,22] that there exists a critical level of cold-deformation for high-silicon electrical steels for which the grain-size of the steel increases many fold after annealing.

Study of recrystallization and grain-growth of high-silicon steels at present can be differentiated into two types as (i) primary recrystallization and normal grain growth and (ii) secondary recrystallization and abnormal grain growth. There exists a critical level of cold deformation for primary recrystallization to occur which results in a bigger grain size. On higher percentage of cold-work and high-temperature of annealing, few grains grow preferentially over the matrix grains in a particular orientation texture in case of a secondary recrystallization [23,24,25,26].

The critical level of deformation depends on several factors like composition and purity of steel, original structure, conditions of deformation and annealing. The critical level of deformation [20,21] for a transformer steel is reported to be within 4-8 pct. With increase in silicon content, the maximum growth of the grains is obtained at lighter reductions.

Fig. 1.9 shows the effect of amount of reduction on magnetic properties and grain-size of transformer sheet. With increasing silicon content the tendency towards coarse-grain formation weakens. In sheets subjected to critical reduction, the total specific losses are decreased considerably and the magnetic induction in strong field is lowered.

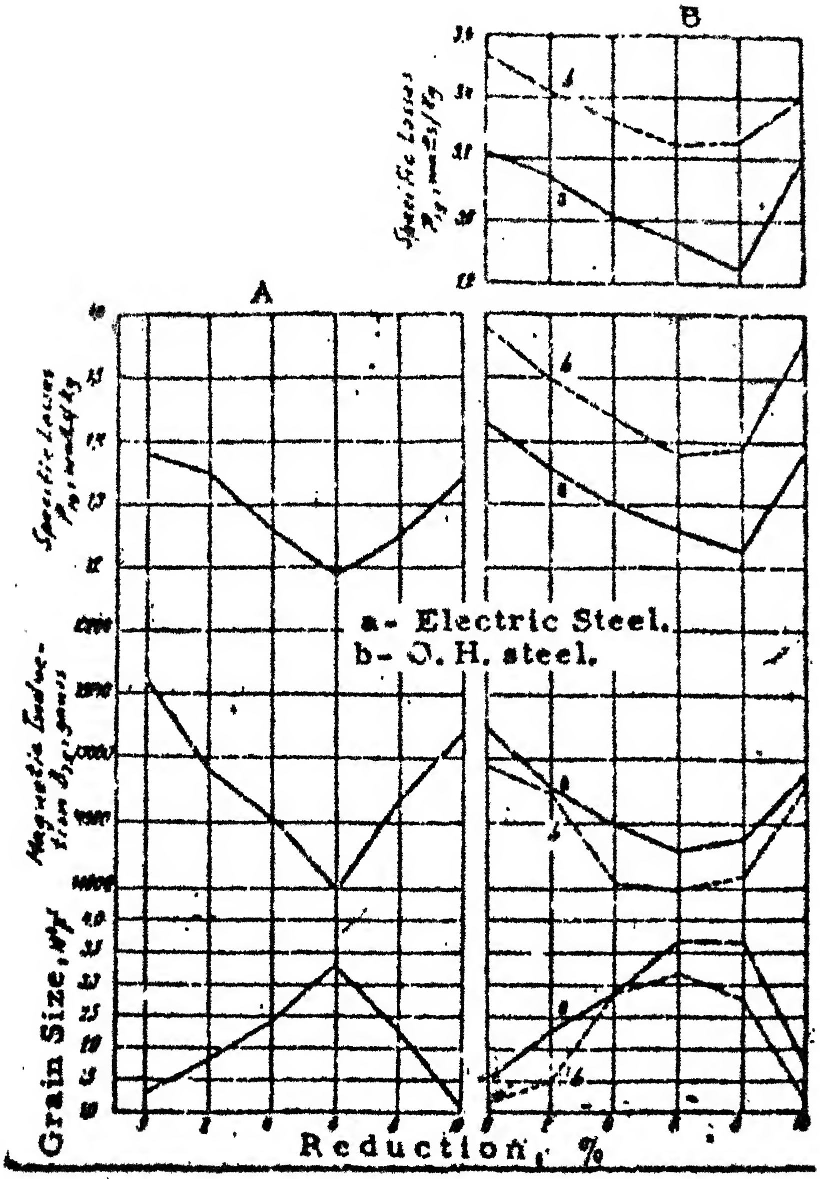

Fig. 1.9. Effect of amount of reduction on magnetic properties and grain size of transformer sheet from laboratory (A) and plant (B) data[21].

Critical cold-deformation at different temperatures have practically identical effects.

The critical reduction does not affect the recrystallization texture or the anisotropy of magnetic properties. Its effect is due purely to change of grain size[21].

Annealing at different temperatures without any deformation causes no particular change in grain-size. The grain becomes finer with increasingly heavier reductions. Correspondingly the core-loss (watt loss) value increases with the increasing percentage reduction beyond the critical value. On annealing above 900°C, the cold working exerts practically no influence on the watt-loss values. Fig. 1.10 shows the watt-loss variation with percentage of cold-reduction and annealing temperature[14].

The internal-strains developed due to cold-work in case of a polycrystalline material can be considered isotropic. The growth of grains is independent of the direction of cold-rolling during primary recrystallization. In a cold-worked matrix, the grains of lower-residual strain energy grow preferentially by consuming grains of higher residual strain[27,28].

Theoretically it is possible to attain a specimen which is a single crystal as it would have the lowest possible

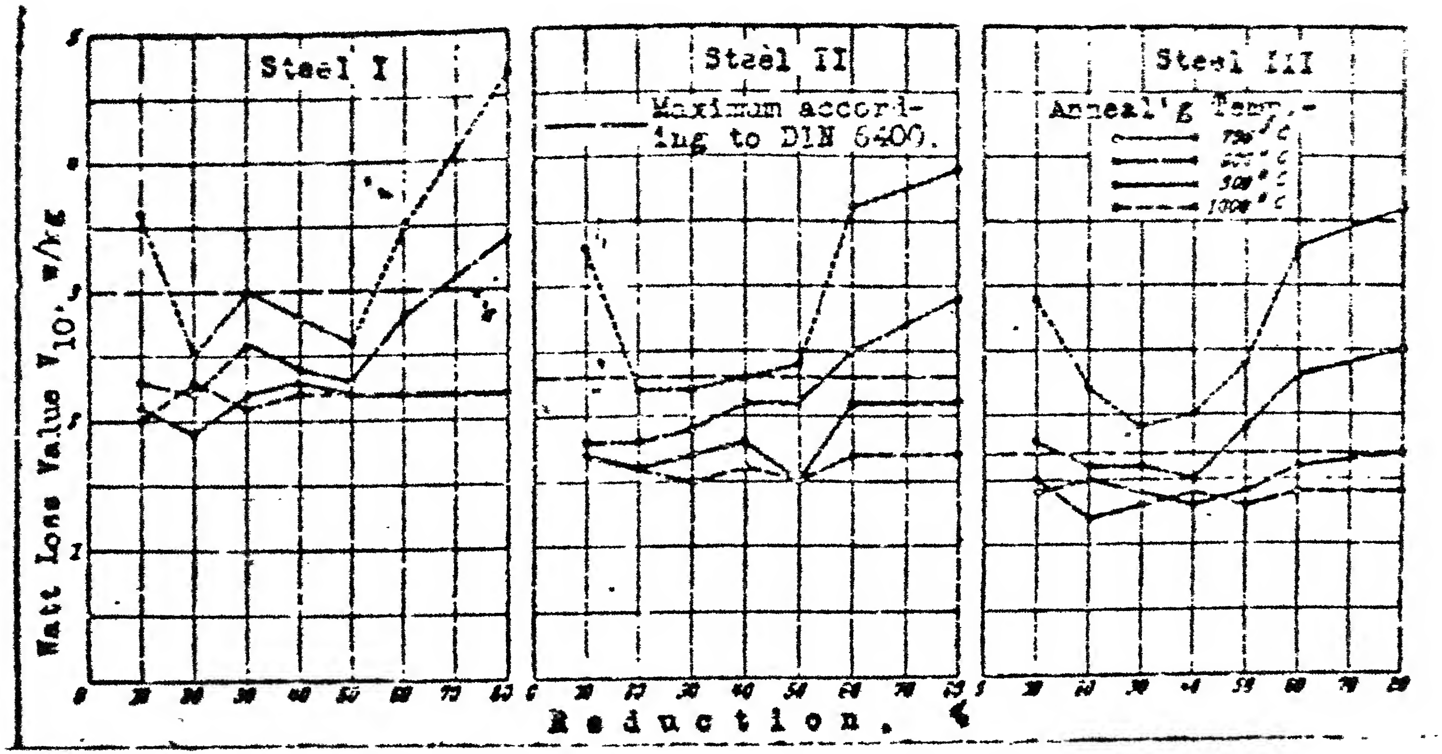

Fig. 1.10. Relationship between watt-loss values and reduction for annealing temperature of 700-1000°C (1290-1830°F)[14]. Gauge - 0.50 mm.

internal energy. But, normal grain-growth is very much restricted due to presence of impurities. The impurities inhibit grain-growth by interacting with the grain boundaries at lower percentage of cold-reduction [29].

I.4 Effect of Chemical Coating on Magnetic Properties

The magnetic properties of electrical grade steels are improved by annealing at high temperatures which causes structural changes depending on the temperature and chemical changes occuring in any particular annealing atmosphere. The best atmosphere for such an annealing treatment is a high vacuum or pure hydrogen [30]. In industrial situations, decarburization is limited due to the lack of penetration of hydrogen inside the packed sheets, whereas in case of vacuum annealing there is not enough oxygen for complete decarburization. To overcome the above difficulties in getting the improvement in the magnetic properties in electrical steels, it is desirable to give a thin chemically-active coating on the sheet or strip prior to annealing.

I.4.1 Characteristics of the Chemical Coatings

The chemical coatings are chosen on the basis of the following characteristics.

i) This should be easily deposited on the sheet surface and should promote decarburization, de-grassing and grain growth of steel and at the sometime prevent its oxidation.

ii) It should prevent sheets sticking together during annealing at high temperatures.

iii) It should leave on the sheet, a thin protective surface film, having good corosion resistance, electrical insulation and a high space factor.

iv) It should improve the magnetic properties of steel.

The use of chemically active coatings to get high electrical insulating property is particularly important is the production of very thin electrical sheets.

I.4.2 Different types of Chemical Coatings

The different chemical coatings which have been tried can be classified into four categories.

a) Chemically neutral and high melting point coatings applied to prevent sticking or welding. These include concentrated talc, finely divided magnesia, alumina, silica, lime etc.

b) Chemically active coatings having comparatively low dissociation temperatures which are suitable for decarburizing,

removing sulphur and other harmful impurities. Among those that have been investigated by various workers[30] are iron oxides, potassium nitrate, calcium and magnesium carbonates. Aqueous sodium hydroxide or phosphoric acid with additions of sodium, potassium, calcium, and barium nitrates, are some of the notable alkaline and non-alkaline oxide-coatings.

c) Coatings which are a mixture of the first and second groups.

d) Organic and semiorganic coatings which induce compressive strains on the sheet surface and there by reduce eddy current loss.

The annealing of transformer grade steel sheets coated with a mixture of magnesia, alumina, and iron-oxides in pure hydrogen atmosphere lowers the percentages of carbon and sulphur to levels as low as 0.005 pct., coarsens the grains, raises the magnetic permeability and lowers the hysteresis loss[31]. It has been suggested that the amount of oxygen in the coating should not be more than 0.005 pct. of the weight of the annealed sheet.

Phosphoric acid, an aqueous solution of magnesia, a mixture of the silicates or oxides of alumina and magnesium with additions of some binders have also been tried.

Electrodeposition using solution of colloidal silica in acetone and even gluing-on of tissue paper have been attempted successfully[32].

Sodium carbonate monohydrate, barium, calcium and magnesium carbonates have been tried as chemically active coatings. They dissociate when heated to 800-1000°C with the liberation of carbon dioxide, promoting the decarburization of transformer sheet.

When the temperature is raised to 1150-1200°C in a vacuum or hydrogen atmosphere, the oxides get reduced to the metallic state. The metal then vapourises and acts as powerful gas scavengers. To prevent the sheet or strip from welding together, those substances were mixed with magnesia. The suspensions used were water, 10 pct. caustic soda or alcohol. When weak solutions of potash is used, no rusty spots were formed and drying time is comparatively shorter[30].

I.4.3 Decarburization of Silicon-Steels:

Removal of carbon from the electrical sheets during annealing is recommended as it is uneconomical to produce steel with extra low carbon content by conventional methods.

The carbon concentration at the metal/scale interface is constant (i.e. in equilibrium with the oxide scale). The

scaling rate can be varied by changing the annealing atmosphere which in turn controls the depth of decarburization.

Decarburization can also occur in atmospheres which do not produce scaling. Such decarburization reactions are as follows:

$$Fe + CO_2 (g) = FeO + CO (g)$$

$$[C] + CO_2 (g) = 2CO (g)$$

$$[C] + FeO = Fe + CO (g)$$

$$[C] + 2H_2 = CH_4 (g)$$

It is evident that the rate of decarburization in the above case is controlled by the CO/CO_2 ratio.

The rate of decarburization depends on the stable phase of steel existing at the prevailing annealing temperature. When the steel is in the ferritic state the diffusion of carbon is very slow due to the very low solubility of carbon in ferrite. In the austenite phase, the decarburization is much faster due to the greater mobile interstitial carbon.

Silicon forms fayalite (Iron silicate) with the iron-oxide in the scale. This reduces the scaling rate. Silicon also increases the activity of carbon and therefore increases the tendency of carbon to diffuse out to the metal/scale interface. The net effect of silicon is thus to increase decarburization[33,34].

I.5 Scope of Present Work:

Iron-silicon alloy of various grades constitute the most of the material used in power electrical apparatus like Transformers, Generators, motors and dynamos. The performance and efficiency of these equipments are controlled by the design and the quality of the material used. A considerable amount of electrical energy is lost due to the employment the material of poor quality which could have been otherwise saved by the use of improved quality material.

The entire range of silicon electrical steel can be broadly classified into transformer-grade where silicon is generally higher than 3 pct. and dynamo-grade using lower silicon percentages upto 3 pct.

Factors affecting the electrical and magnetic properties are mostly chemical composition and the finishing treatment of the steel. It is rather a costly and difficult proposition to achieve very low levels of residual impurities at the steel making stage. Considerable interest has been shown in the development of electrical grade steels, for transformers however very little work has been reported in the case of dynamograde steel. It was considered that some of the techniques used in improving the electrical properties of transformer grade steels, such as recrystallization-grain growth

and the application of chemically active coatings prior to annealing, could also be applied to dynamograde steels. With this in view the present investigation covers the development of property improvements of 300-grade silicon-steel sheets in two parts viz through the critical cold reduction followed by annealing and also through the application of chemically active coating over the sheet surface.

CHAPTER II

EXPERIMENTAL PROCEDURE

II.1 Sample Preparation

II.1.1 Sample Selection

Hot rolled 300 grade silicon-steel sheets used for dynamos were selected for the purpose of conducting the experiments. The sheets selected correspond to the middle of the packs covering two different thicknesses respectively. The ladle sample analysis (L.S.A.) for the two thickness sizes are given below.

	L.S.A. pct.				
Thickness	C	Si	Mn	P	S
1.00 mm	0.03	1.42	0.46	0.019	0.029
0.50 mm	0.08	1.48	0.45	0.018	0.032

The complete processing detail for the above sheets is given in Fig. 2.1.

Steel-Ingot

↓

Rolled in 46" Blooming mill

↓

Rolled in 32" mill and 24" continuous
mill to sheet bars (width - 305 mm)

↓

Sheet Bars cold sheared to cut Bars
(952.5 mm long)

↓

Heated in Bar furnace to 950°C

↓

Rolled in 3-high Roughing mill

↓

Heated in packs of 2 to 4 in continuous furnace
at 1000°C

↓

Thickness reduced in the 2-high finishing-
mill and then packs opened.

↓

Opened sheets again folded for doubling
and packs are heated in a continuous
pack furnace to 1000°C/1050°C

↓

Rolled in the finishing mill to the
final section thickness.

↓

Trimmed to the order size.

Fig. 2.1 Processing of 300-grade silicon-steel
from ingot stage to trimmed sheets
stage.

II.1.2 Cold-Reduction

Sheets of 1.0 mm thickness were selected for the study of effect of cold-rolling. Initially the bigger sheets were sheared into smaller sizes of 350 x 150 mm dimensions. This size was dictated by the limitations of the laboratory rolling mill. Half of the sheets were cut parallel to the rolling direction and the remaining half in the transverse direction. The length and width of each piece of sheets were measured accurate to 0.5 mm. The sheet pieces were then subjected to nominal cold reduction of 5 pct., 10 pct. and 20 pct. respectively. The exact cold reduction percentage was calculated from the change in length after cold-rolling assuming the change in width to be negligible.

$$\% \text{ cold-reduction} = \frac{A_1 - A_2}{A_1} \times 100 \qquad \ldots(i)$$

and $$A_1 \times L_1 = A_2 \times L_2 \qquad \ldots(ii)$$

where, A_1, L_1 are the area of cross-section, and length respectively before rolling.

and , A_2, L_2 are the area of cross-section and length respectively after rolling.

from equation (ii),

$$\frac{A_2}{A_1} = \frac{L_1}{L_2}$$

on substitution in eqn. (i)

$$\% \text{ cold-reduction} = \frac{A_1 - A_2}{A_1} \times 100 = (1 - \frac{A_2}{A_1}) \times 100$$

or,

$$\% \text{ cold-reduction} = (1 - \frac{L_1}{L_2}) \times 100 = \frac{L_2 - L_1}{L_2} \times 100 \qquad \ldots \text{(iii)}$$

The percentage cold reduction was adjusted within $\pm$ 10 % of the nominal value.

II.1.3 Shearing of Samples

Samples for the measurement of core-loss by Epstein-square test were sheared in a power shear. Each set of samples contained strips of 305 mm x 30 mm size, half of which were cut parallel to the rolling direction and the remaining half cut perpendicular to the rolling direction according to IS : 649-1963. In case of 1.0 mm thick sheets, 8 pieces were taken (4 in the parallel and 4 in the perpendicular direction), while in case of 0.5 mm thick sheets, 12 pieces were taken (6 in parallel and 6 in perpendicular direction) in all.

II.1.4 Pickling

The oxide layer which was present on the surface of the sample strips was removed by pickling in 50 pct. dilute hydrochloric acid for about 30 minutes and a bright surface was obtained. After pickling, the strips were thoroughly scrubbed and washed in water. To prevent rusting, the strips after washing were immediately dipped in acetone and dried quickly using a blower. The loss in weight after pickling was found to be between 2-4 pct.

II.1.5 Chemical Coatings

For the study of chemical coatings, sheets of 0.50 mm thickness were selected as the effect of coatings observed is better due to faster diffusion, when the thickness of the sheets is low. Five different chemical coatings were investigated. Table II.1 gives their composition by weight percents. Initially the individual compounds constituting any coating were weighed separately and then dry mixed in a mortar and pastel set. Water was then added to the dry mix to get a suspension consistent enough to give an uniform coating to the pickled strips when dipped.

Coated strips were spread over enamelled trays and dried in hot air with the help of a blower. Final drying

of the coated samples was done over-night in an electric-oven set at a temperature of 150°C. Table II-2 gives the approximate weight of the chemical-coating for various coated samples. All the coated samples were identified properly to avoid any possible mix-up during subsequent treatments.

Table II.1 Chemical Coatings and their Composition

Coating No.	Components	Composition in wt. pct.
0	No coating	--
1	$MgCO_3$	100
2	$BaCO_3 + MgO + KOH$	30 : 30 : 40
3	$CaCO_3 + MgO + KOH$	30 : 30 : 40
4	$NaCl + MgO + KOH$	30 : 30 : 40
5	$Na_2CO_3.H_2O + MgO$	50 : 50

Table II.2 Amount of Coatings on Silicon-steel in gm/sq.meter

Coating No.	Weight of coating/ set of samples in gms	Weight of coating in gms/sq. meter	Remarks
1	12-15	55-70	Resulted in rusty spots.
2	30-35	140-160	-
3	30-35	140-160	-
4	35-40	160-180	-
5	18-20	80-90	Coating was uneven

II.2 Annealing Treatment

II.2.1 Experimental Set-up

Annealing of strip samples was carried out in an electric tubular furnace heated by silicon-carbide resistors. Temperature of the furnace could be controlled within ± 10 °C. Different controlled atmospheres were used like hydrogen, nitrogen and vacuum. When annealing in nitrogen or hydrogen, the gas was purified by passing it through traps containing fused calcium-chloride for adsorption of moisture and alkaline pyrogallol solution for the adsorption of oxygen (O_2) and carbon dioxide (CO_2). The quantity of gas consumed was metered using a gas flow meter. When annealing in vacuum, one end of the furnace tube was sealed and the other end was connected to a rotary vacuum pump through vacuum pressure hose. The order of vacuum was monitored continuously using a thermocouple gauge which could measure vacuum up to 10 microns.

Fig. 2.2 and Fig. 2.3 show the furnace set-up for annealing in gas atmosphere and vacuum respectively.

II.2.2 Annealing Cycle

For the samples cold rolled, annealing temperatures, selected were 700 °C, 800 °C and 900 °C respectively while for

Fig. 2.2. Experimental set-up for annealing in a gas atmosphere.

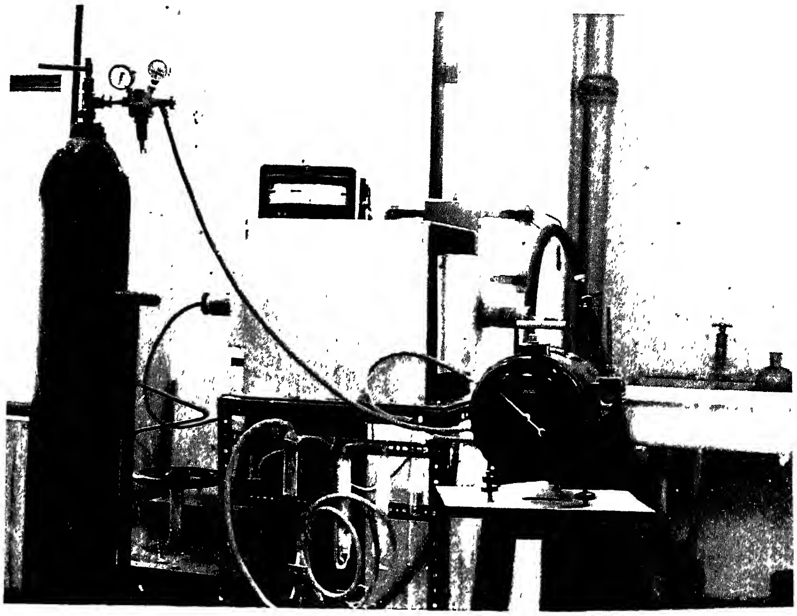

Fig. 2.3. Experimental set-up for annealing in vacuum.

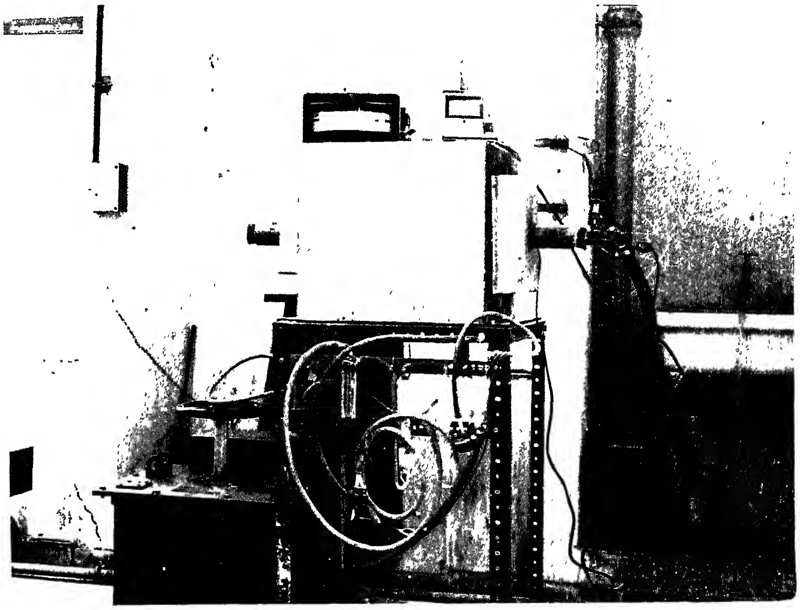

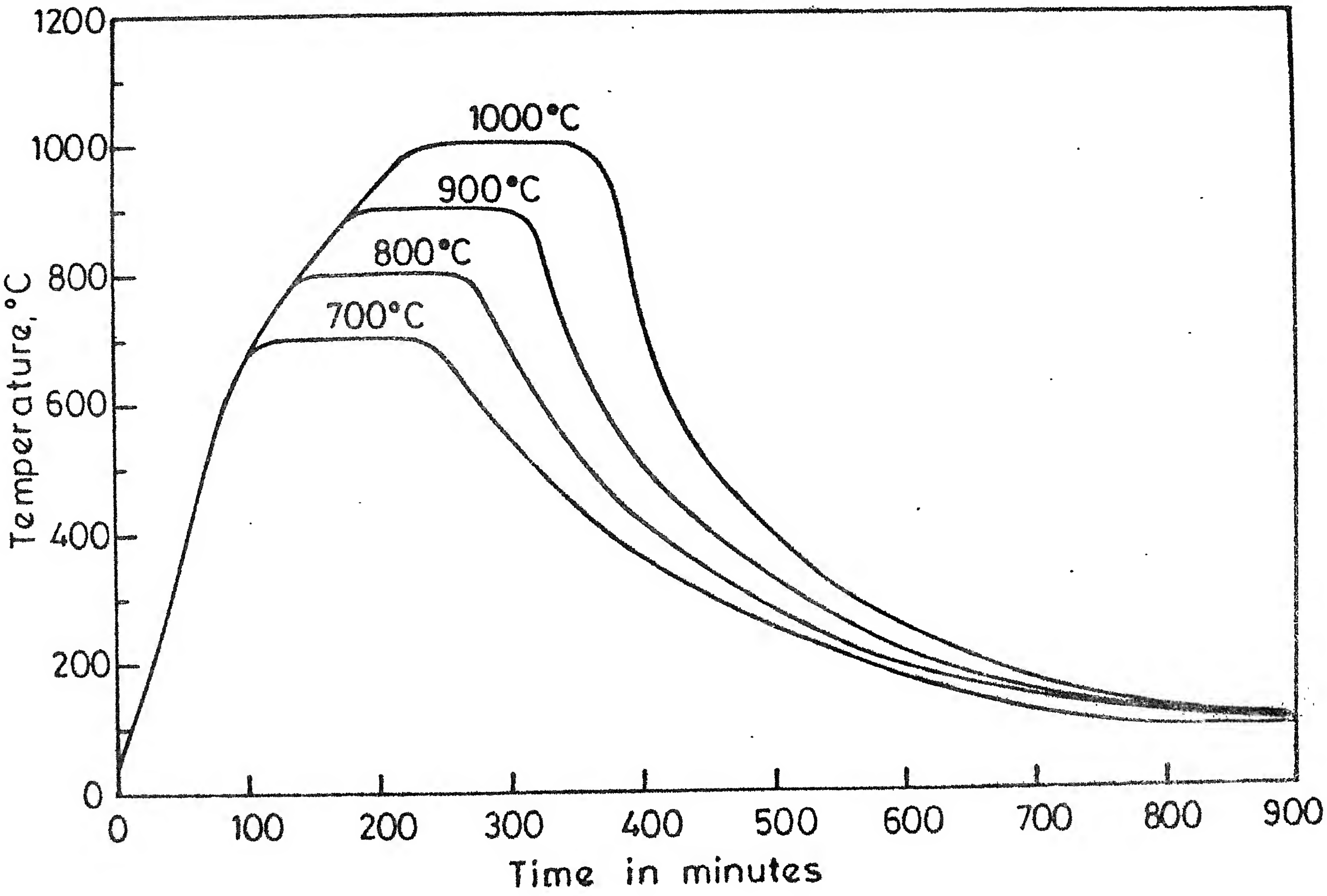

Fig. 2.4 - Various annealing cycles.
(annealing atmosphere - hydrogen)

the chemically coated samples, temperatures used were 800°C, 900°C and 1000°C respectively. Higher annealing temperatures in case of coated samples were chosen after considering the different decomposition temperatures of the coating compounds. Socking time was maintained for 2 hours in all the cases. Fig. 2.4 gives the annealing cycle for annealing in hydrogen atmosphere for different temperatures.

When annealing the coated samples, those corresponding to nos. 1, 2 and 3 were annealed in a group. Samples coated with coating nos. 4 and 5 were grouped together separately during annealing while uncoated samples were annealed individually. In case of vacuum annealing of the samples, coated with coatings 4 and 5, it was observed that sodium was getting deposited towards the ends of the furnace tube wall. These deposits used to catch fire due to exposure to the atmospheric moistair during the removal of the samples from the furnace after annealing. This created an unsafe condition for which the experiments in vacuum could not be completed.

II.3 Measurement of Electrical and Magnetic Properties

The electrical and magnetic properties of the annealed samples were measured according to IS : 649-1963.

II.3.1 Core-loss Measurement

Core-loss at a frequency of 50 Hz and 1 Weber/sq. meter magnetic induction, was measured in terms of Watts/kg, using an Epstein-square testing machine in the Metallurgical Division of the Tata Iron and Steel Co. Ltd., Jamshedpur. The testing machine essentially uses the principle of a transformer. The samples are inserted into the slots of the Epstein-square frame and are formed into a complete magnetic circuit. The slots are inside coils which form the primary and the secondary of a transformer. When current at specified voltage (calculated from the weight of the sample) is applied, the watt meter reads the power loss in watts inside the frame. This power-loss is then converted into watt loss per kg of the sample. Fig. 2.5 shows the assembly of a Epstein-square testing machine.

The core-loss values in case of cold-rolled samples were corrected for the difference in sample thickness with the help of Fig. 2.6. This graph was plotted using the data available in IS: 648-1970.

II.3.2 Initial Magnetization Curve

The same samples used for the core-loss measurements in the Epstein-square test were used for finding out the

Fig. 2.5. Assembly for core-loss measurement according to Epstein-square method.

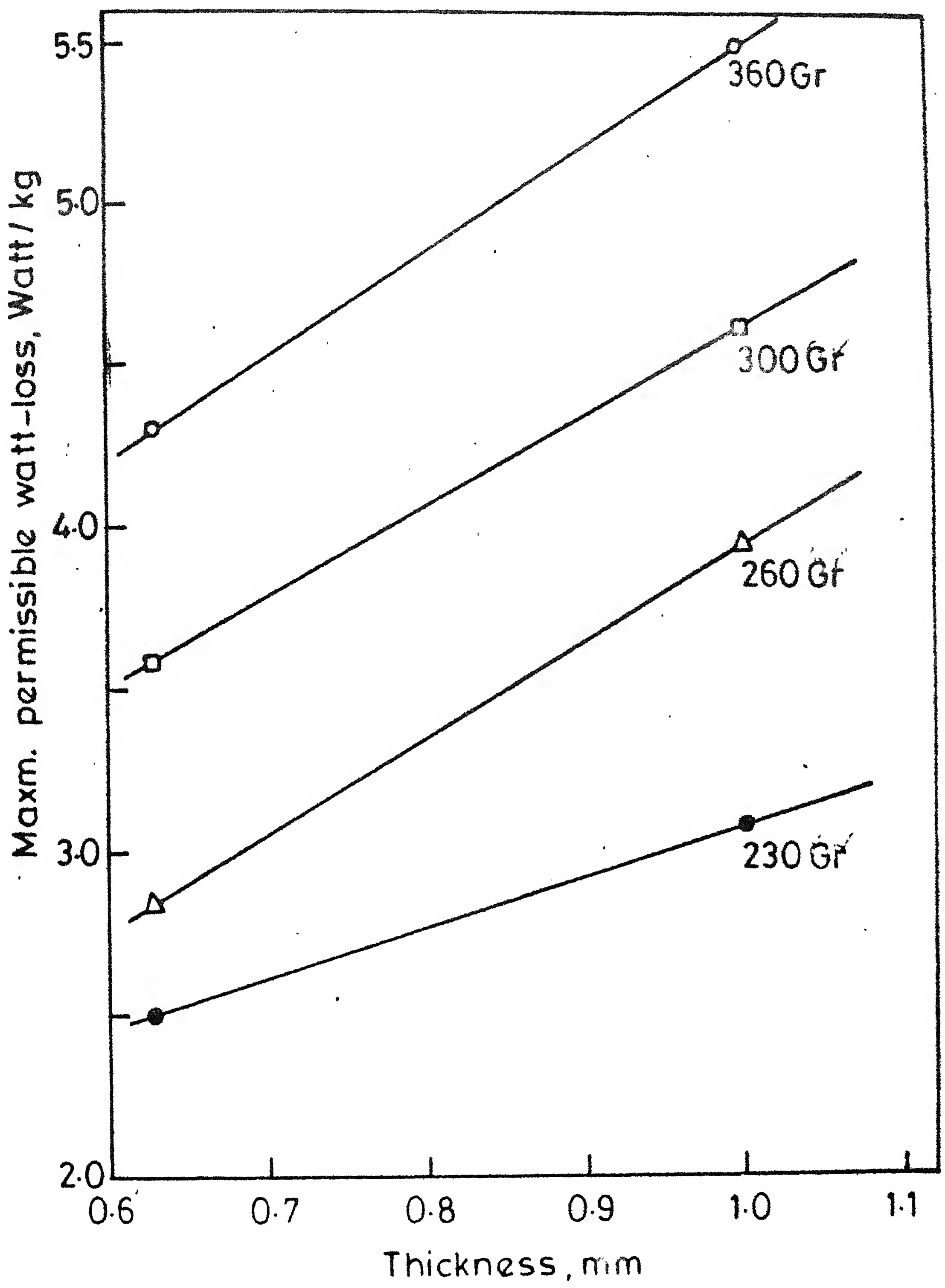

Fig. 2.6. Variation in maximum permissible core-loss with respect to thickness of various grades of silicon steel sheets (After IS : 649).

initial magnetization characteristics. The machine used was Fahy's simplex permeameter. This is essentially a ballistic galvanometer set-up where the samples are clamped inside a yoke having both magnetizing and sensing coils. For any current in the coil, both the magnetic field and induction are monitored from the deflection in the lamp and scale arrangement. Fig. 2.7 is a photograph of Fahy's simplex permeater set-up used in the present investigation.

The initial magnetization curve (induction, B, in Wb/m^2 vs. field, H, in Amp. Turns/meter, A/m) was plotted from the deflection values. The maximum permeability (μ_{max}) was calculated by taking the field and corrected induction values ($\mu = \frac{B}{H}$). B at 800 A/m field was also foundout from the magnetization curve. This B values at 800 A/m field also give some idea regarding the magnetizing characteristics of the sheets.

II.4 Optical Microscopy

II.4.1 Sample Preparation

After the electrical and magnetic tests were completed, one strip from the middle of each set of samples was selected for the purpose of micro-structural examination. Samples for the microscopic study were cut (about 15 mm long) from

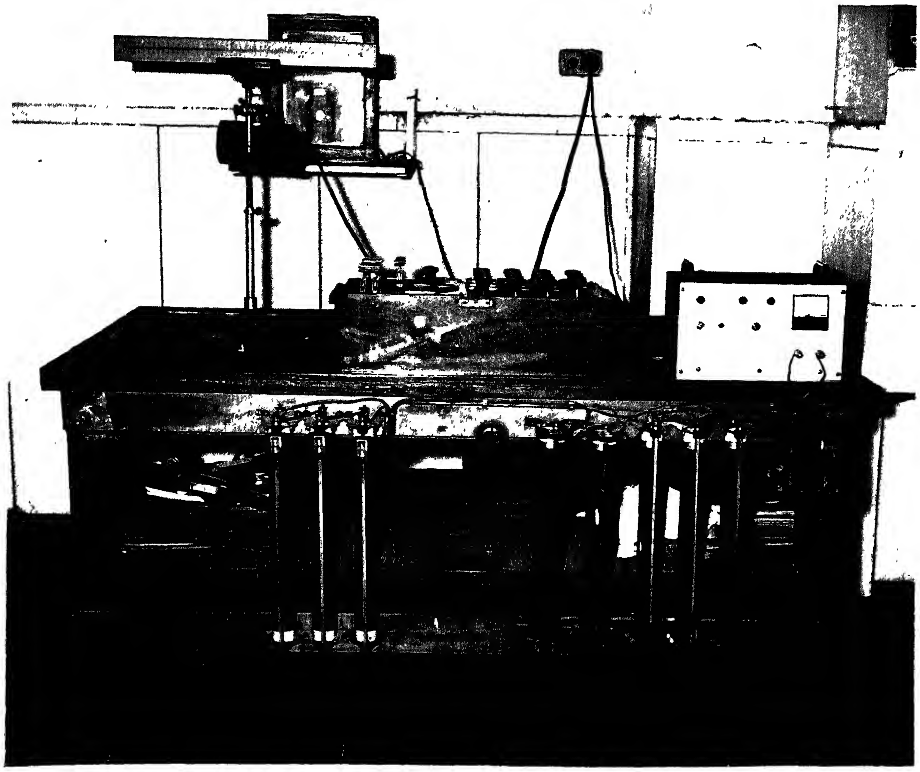

Fig. 2.7. Fahy's Simplex permeameter assembly.

the central portion of each strip and were mounted on bakelite, so that all the three cross-sectional planes were available for examination individually.

The polishing of the mounted samples was done in the usual manner going through the steps of initial grinding on linser belt, polishing on various grades of emery paper, and final polishing on wheel using lavigated alumina powder of size 2 μm. Etching of polished specimens was done using 3 pct. Nital solution.

II.4.2 Microstructure

Optical microscopic examination of the various samples was done on 'Neophot-21' metallograph. Typical photomicrographs of the different samples already enumerated were taken at a magnification of 100.

II.4.3 Grainsize and Aspectratio Measurement

In case of cold-rolled samples the average grain size along the three perpendicular directions were measured by the intercept method. The arithmetic mean of the average grain sizes along the three axes (from the three sections) was represented as the average grain size[35], Grain aspect ratio in the rolling-plane of the grains was found out by taking the ratio of the average grain size along and across the rolling direction.

In case of chemically coated samples, the average grain size was also measured by the intercept method over the section parallel to the rolling plane.

II.5 Brittleness Test

Brittleness of the strips was determined by the number of reverse bends (from + 90^{0} to - 90^{0}) till signs of fracture appeared as per Indian standard IS: 649-1963. A α-Ductilometer (Fig. 2.8) was used for this purpose. Samples of 10 mm width and 100 mm length cut from the strips parallel to the direction of rolling used for this testing.

II.6 Chemical Analysis

After all the tests were conducted, drillings from the Epstein-square samples were taken for chemical analysis. Elements like Si, Mn, S, P were determined using wet-method of analysis and carbon was determined by combustion method using 'sterling apparatus'.

Fig. 2.8. α-Ductilometer set-up.

CHAPTER III

RESULTS

Part I

Cold-Worked and Annealed Silicon-Steel Sheets

III.1 Microstructure

Fig. 3.1 shows the microstructure of as hot-rolled sheets. Elongated ferrite grains are clearly visible which indicate that the recrystallization during hot-rolling was incomplete.

Fig. 3.2 shows the microstructure of steels cold worked to various extents and annealed in hydrogen at temperatures of 700°C, 800°C and 900°C respectively. The grains of 10 pct. cold-worked sheets are larger than any other cold worked samples after annealing at any temperature.

Fig. 3.3 and Fig. 3.4 show the microstructure of steels cold-worked and annealed at 800°C in vacuum and nitrogen atmosphere respectively. The grains are larger at 10 pct. cold-reduction as observed in case of hydrogen atmosphere.

Fig. 3.5 shows the microstructure of steels cold-worked and annealed in hydrogen atmosphere at 800°C. The

(i) in the plane parallel to the rolling direction and perpendicular to the rolling plane (1.0 mm thick sheet).

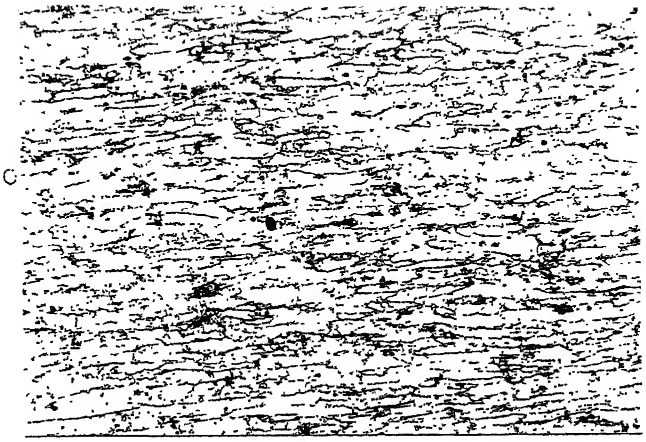

(ii) in the plane parallel to the rolling plane (0.5 mm thick sheet)

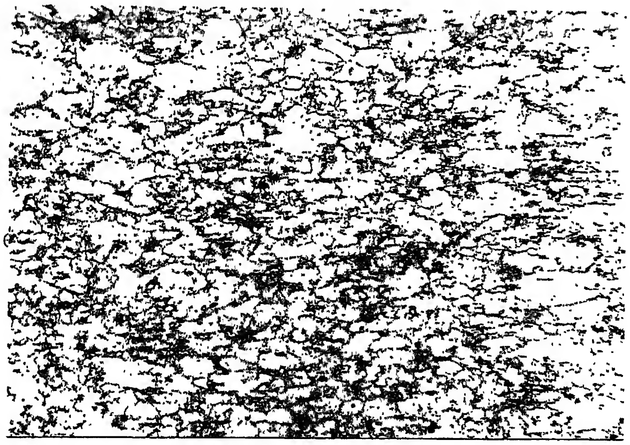

Fig. 3.1 Microstructure of as received 300 grade silicon-steel sheet (As hot rolled).

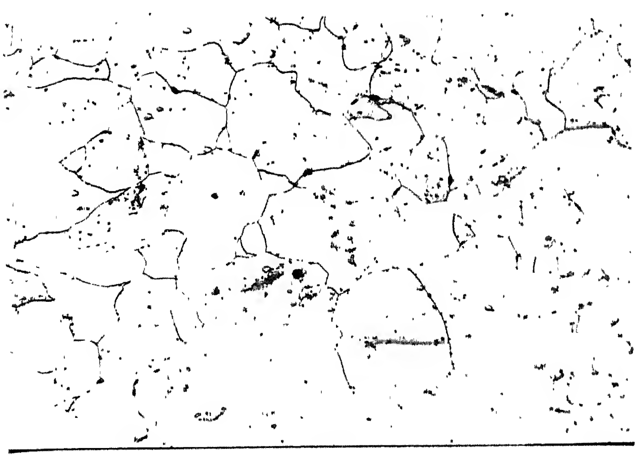

Cold-redn. 0 pct.

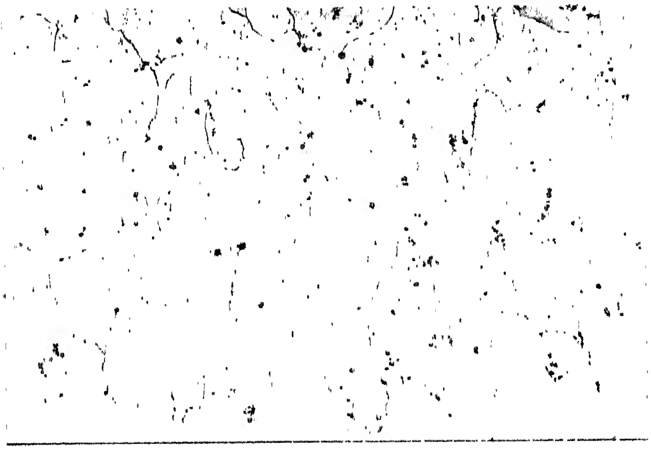

Cold-redn. 5 pct.

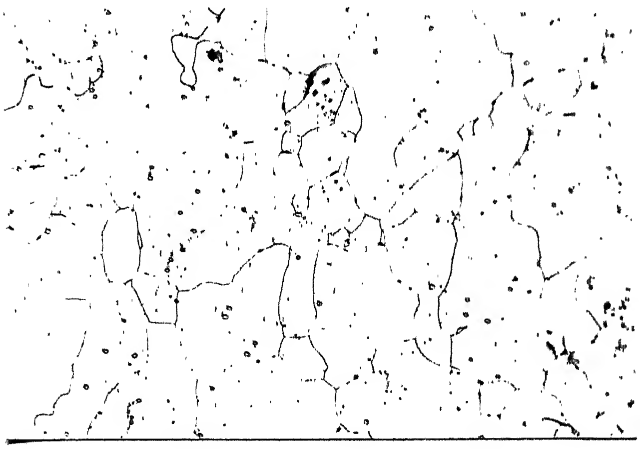

Cold-redn. 10 pct.

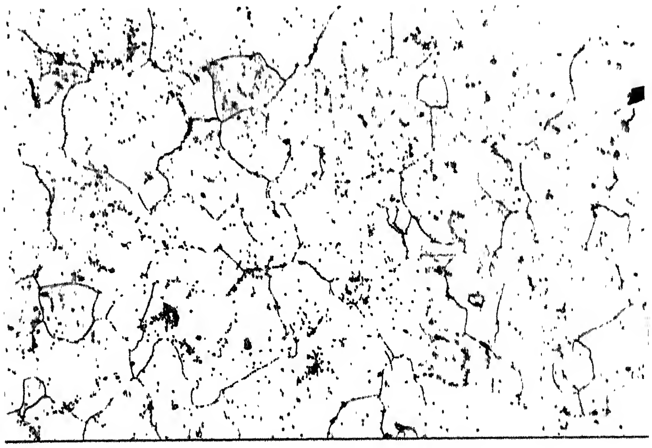

Cold-redn. 20 pct.

Fig. 3.2. Microstructures of annealed 300 grade silicon-steel sheet after different cold reductions.

(All in a plane parallel to rolling plane) X 100

(a) Annealed at 700°C for 2 hrs. in hydrogen.

Fig. 3.2 (Contd.)

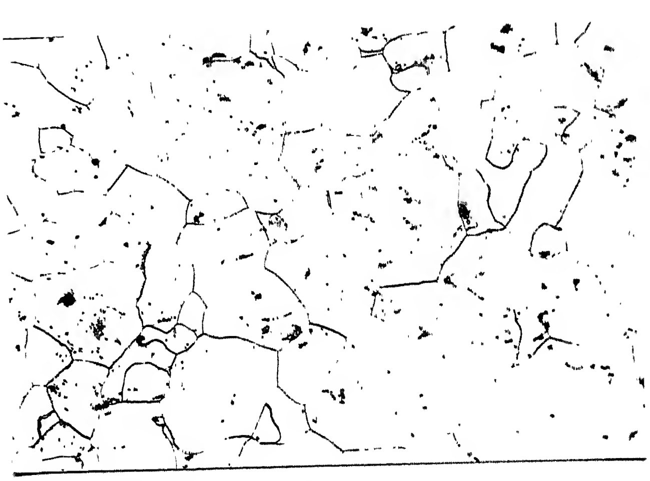

Cold-redn. 0 pct.

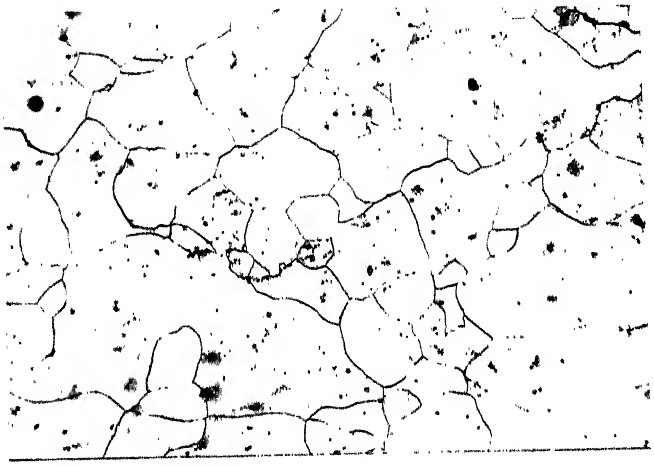

Cold-redn. 5 pct.

Cold-redn. 10 pct.

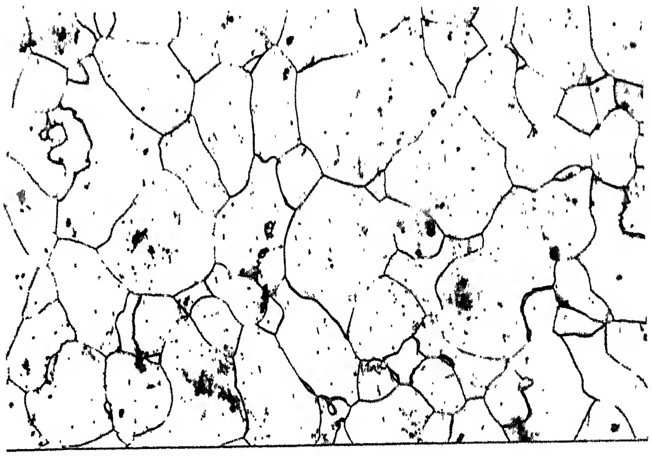

Cold-redn. 20 pct.

(All in a plane parallel to rolling plane) X 100

(b) Annealed at 800°C for 2 hours in hydrogen

Fig. 3.2 (Contd.)

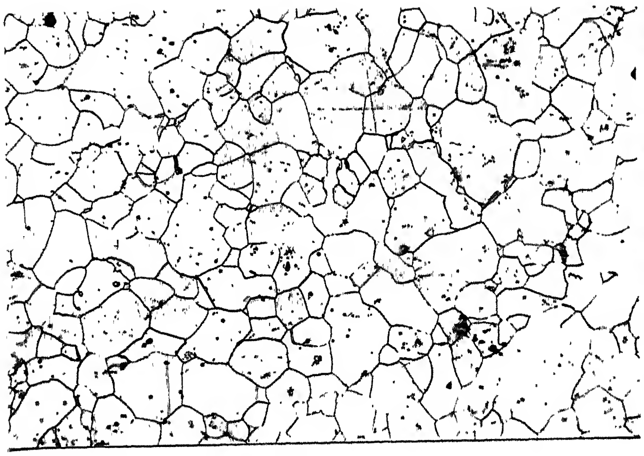

Cold-redn. 0 pct.

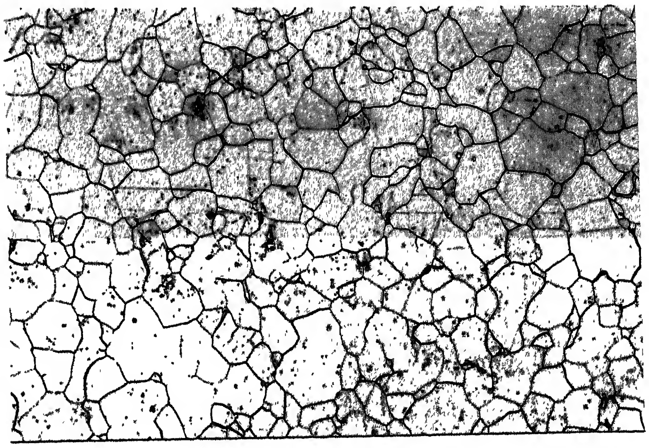

Cold-redn. 5 pct.

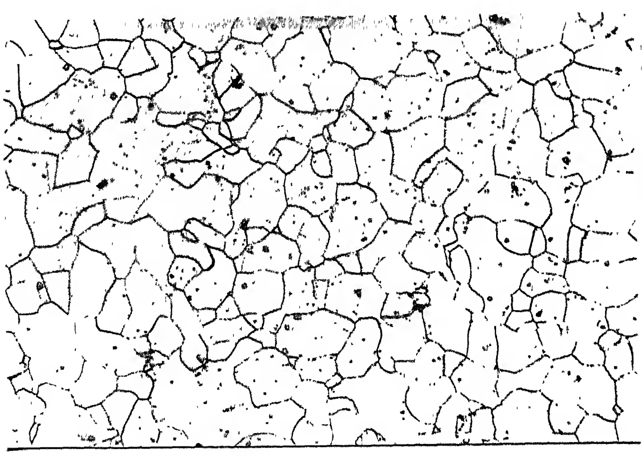

Cold-redn. 10 pct.

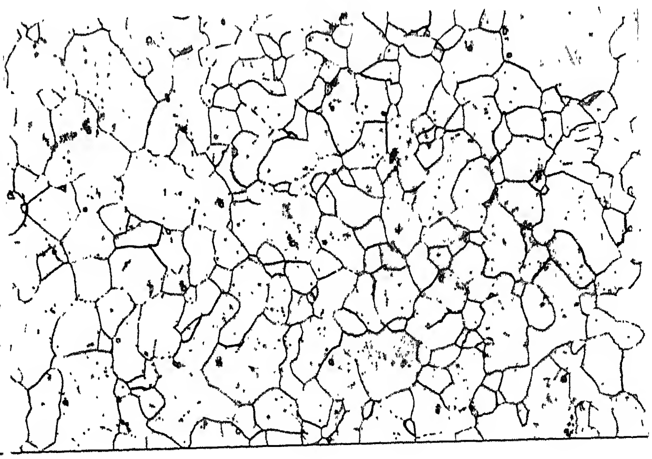

Cold-redn. 20 pct.

(All in a plane parallel to rolling plane) X 100

(c) Annealed at 900°C for 2 hours in hydrogen

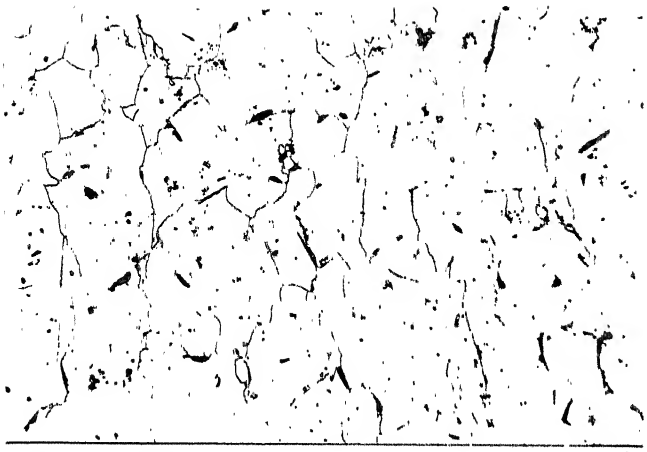

Cold-redn. 0 pct.

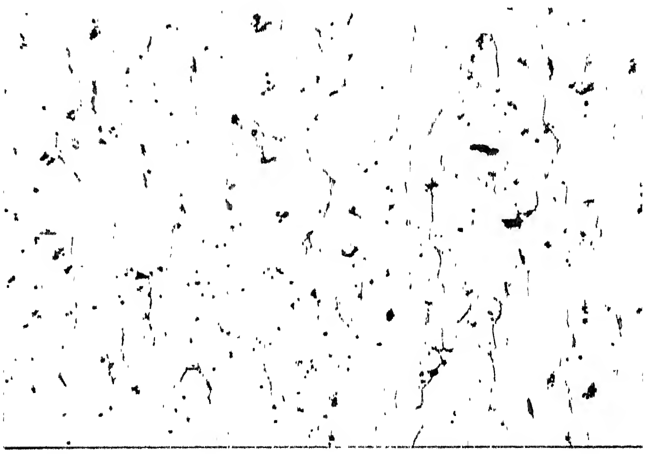

Cold-redn. 5 pct.

Cold-redn. 10 pct.

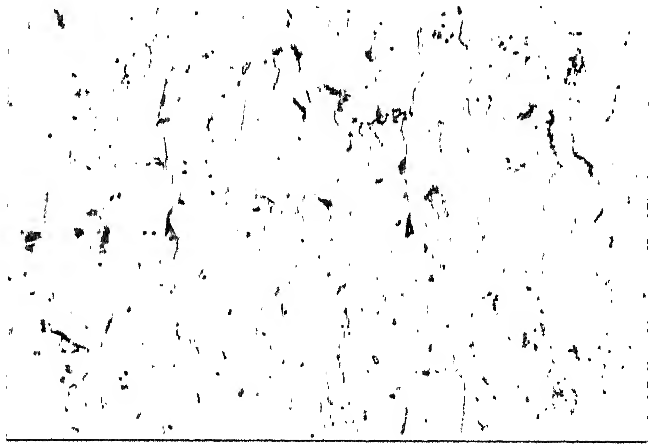

Cold-redn. 20 pct.

Fig. 3.3. Microstructures of 300 grade silicon-steel cold worked and annealed at 800°C for 2 hours in nitrogen atmosphere. (In a plane parallel to rolling plane) X 100.

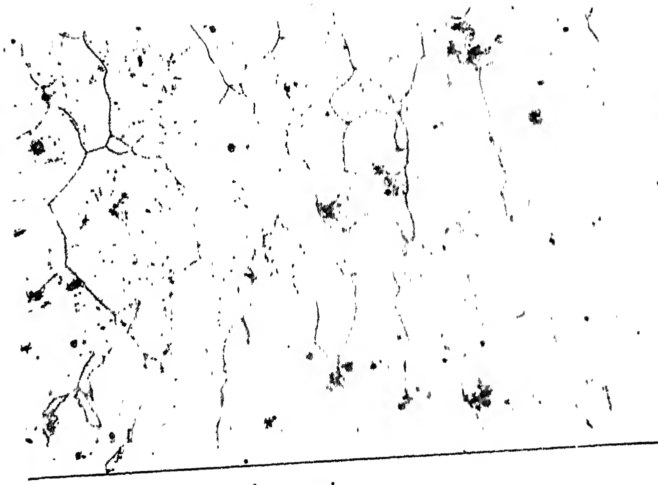

Cold-redn. 0 pct.

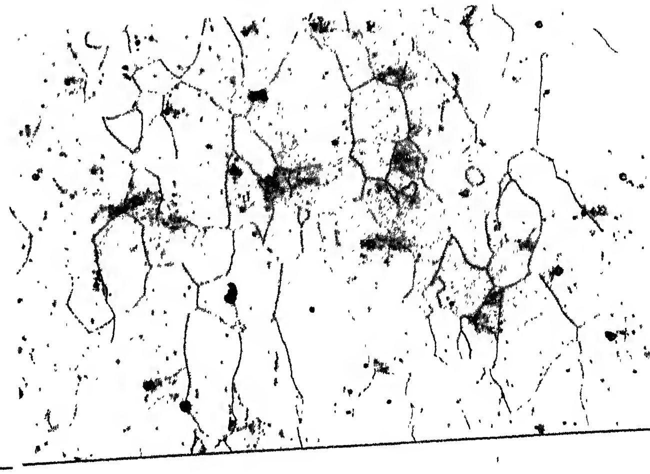

Cold-redn. 5 pct.

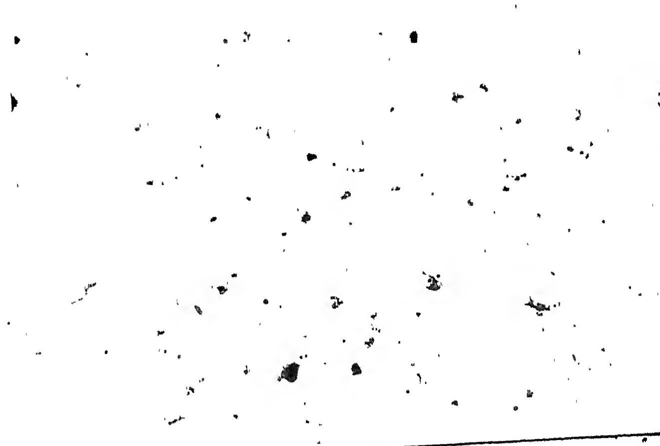

Cold-redn. 10 pct.

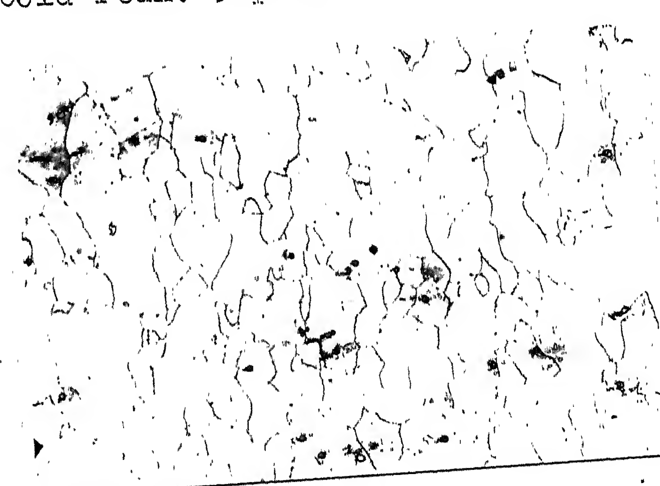

Cold-redn. 20 pct.

Fig. 3.4. Microstructures of 3.0 grade silicon-steel cold worked and annealed at 800°C for 2 hours in vacuum (In a plane parallel to rolling plane) X 100.

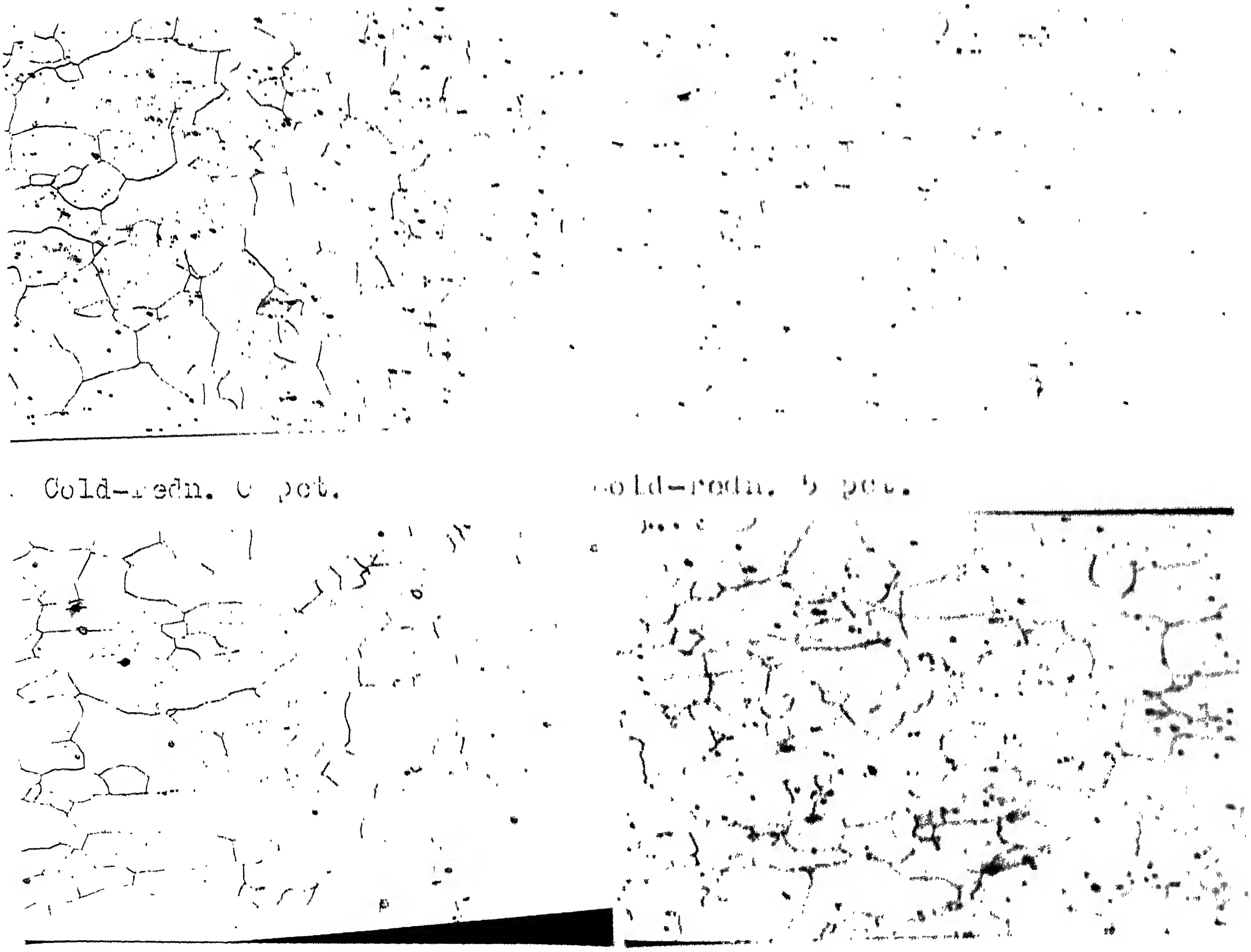

Cold-redn. 0 pct. Cold-redn. 5 pct.

Cold-redn. 10 pct. Cold-redn. 20 pct.

Fig. 3.5. Microstructures of 3.0 grade silicon-steel cold worked and annealed at [illegible] for 2 hours in hydrogen atmosphere. (In a plane perpendicular to rolling plane, but parallel to rolling direction) x 100.

micro-section is in a plane perpendicular to the rolling plane and in a direction parallel to the rolling direction. The structure constitutes of elongated grains.

The microstructure in all the above cases is ferritic with distinct grain boundaries. There was no detectable precipitation of carbides when examined even at a magnification of 1000.

III.2 Grain Size

Fig. 3.6 shows the variation of average grain size with respect to different levels of cold working for different temperatures and atmospheres of annealing. For any annealing atmosphere the critical cold-reduction is 10 pct. for which the grain size of the steel is maximum. With the increase in cold reduction upto 20 pct. the grain size falls down. The grain size with respect to annealing temperature variation shows the descending order of grain size in the order $800 \rightarrow 700 \rightarrow 900^{\circ}C$ for any annealing atmosphere or cold-reduction. On the whole the grain coarsening is maximum in case of vacuum annealing as compared to the other annealing atmospheres such as hydrogen and nitrogen.

The magnitudes of grain-size of the sheets where cold working was done in parallel and perpendicular to the hot-rolling directions are approximately similar. Fig. 3.7

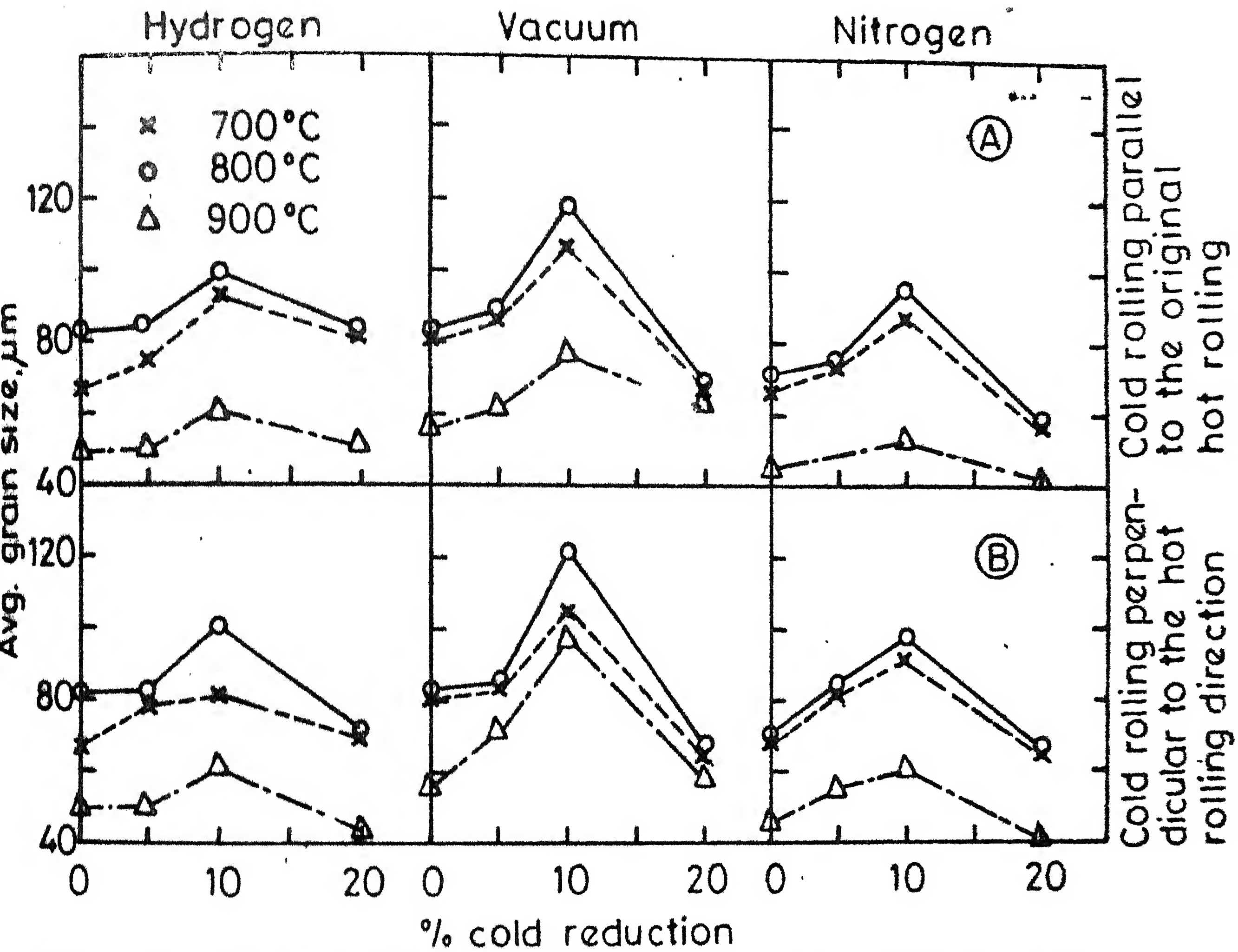

Fig. 3.6. Average grain-size variation of 300 grade Si-steel cold worked and annealed in various atmospheres.

(A) Cold-rolling parallel to hot rolling direction

(B) Cold-rolling perpendicular to hot-rolling direction.

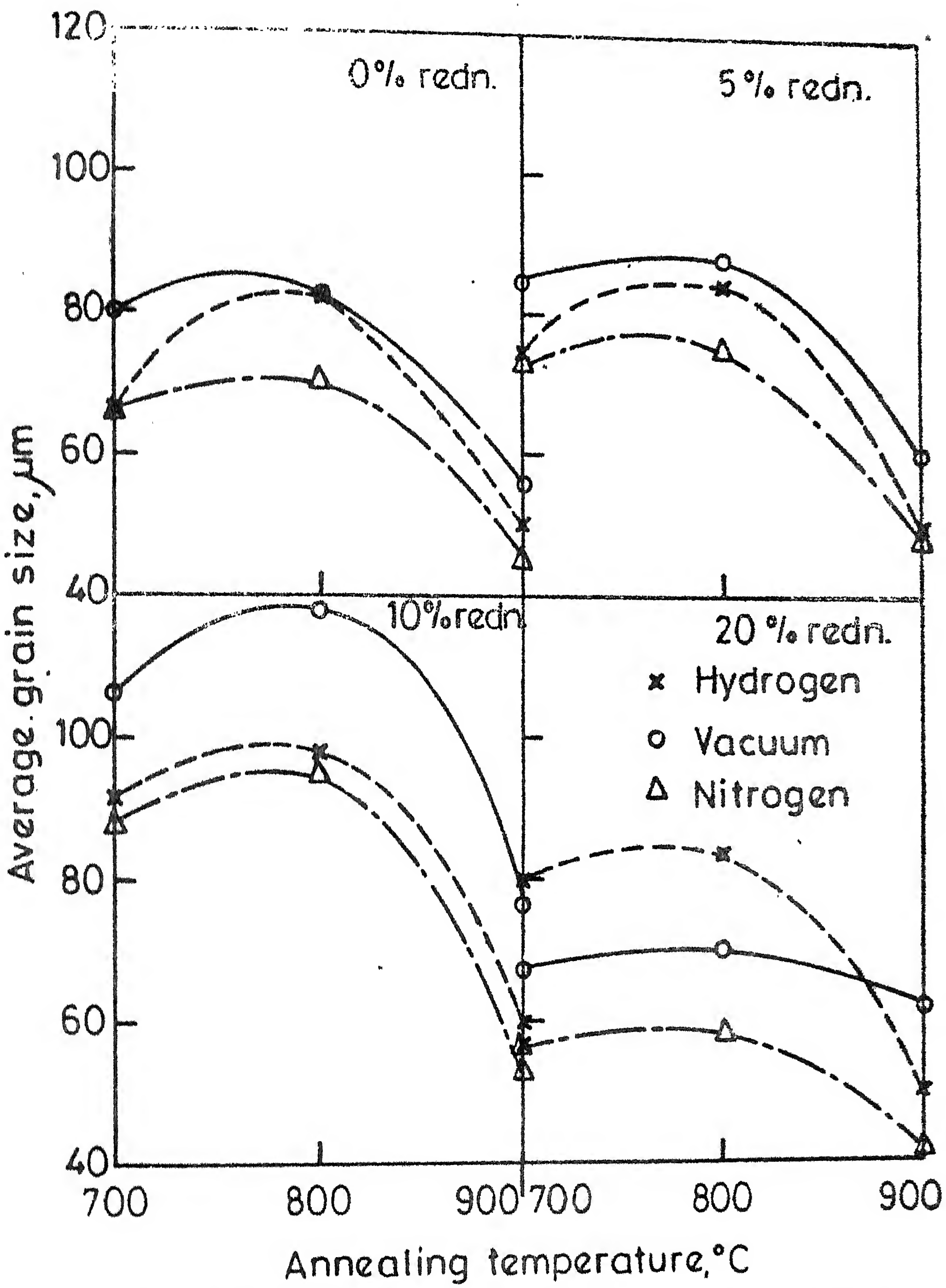

Fig. 3.7. Average grain-size variation of 300 grade Si-steel cold worked and annealed at different temperatures in various atmospheres (cold-rolling done in a direction parallel to hot-rolling direction).

shows the variation of grain size with respect to annealing temperature and atmosphere for any particular percentage of cold-reduction.

III.3 Grain Aspect-Ratio

Fig. 3.8 shows the variation of grain aspect-ratio of cold worked sheets, when measured along the cold rolling plane. This variation was determined in both cases of cold reduction i.e., perpendicular to or parallel to hot-rolling direction. In case of hydrogen and nitrogen atmosphere annealing, the aspect ratio of grains for any level of cold work increases in the order 900 → 800 → 700°C, whereas in case of vacuum annealing this trend is not consistent. Any increase in the level of cold reduction increases the aspect ratio of the grains. Aspect ratio of grains when subjected to cold reduction perpendicular to hot rolling direction approaches a value of unit much faster as compared to those subjected to cold-reduction parallel to the hot-rolling direction.

III.4 Core-loss

Fig. 3.9 shows the measured core-loss variation for cold-worked silicon-steels annealed at various temperatures and in different atmospheres. The core loss for any cold work

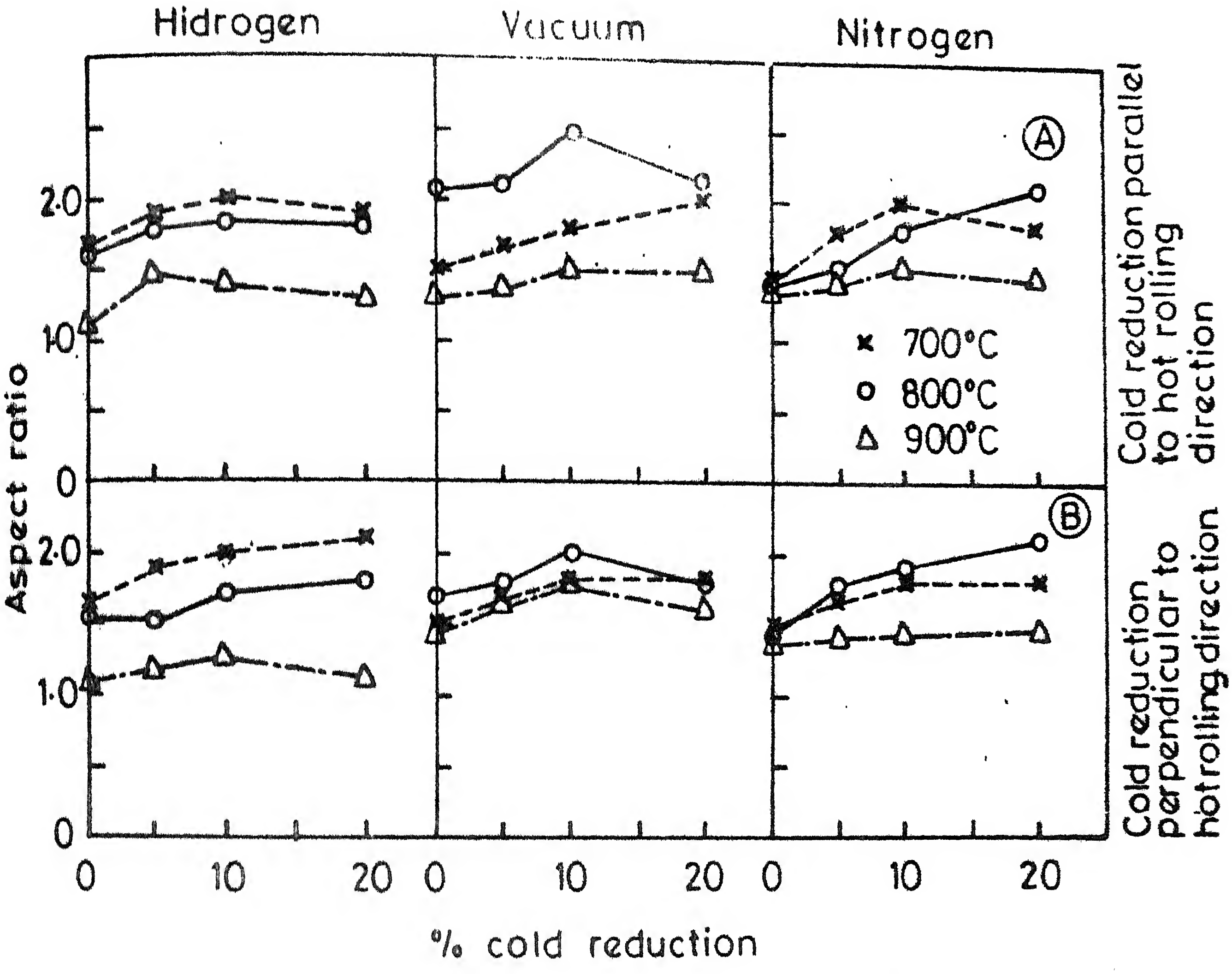

Fig. 3.8. Grain aspect ratios of 300 grade Si-steel Cold-rolled and annealed in various atmospheres.

(A) Cold-rolling parallel to hot-rolling direction.

(B) Cold-rolling perpendicular to hot-rolling (micro-section perpendicular to rolling plane and parallel to rolling direction).

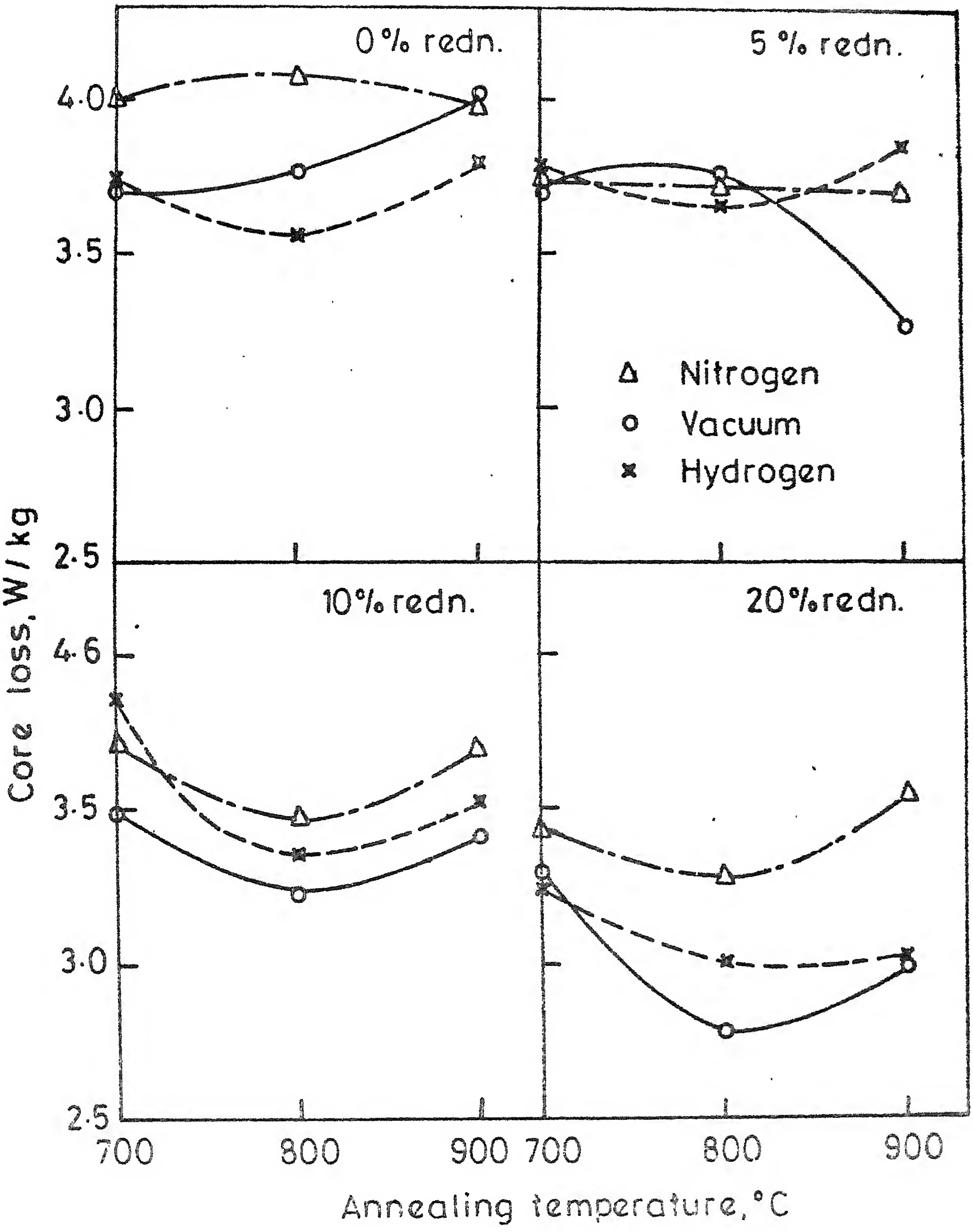

Fig. 3.9. Core loss variation of cold-worked 300 grade Si-steel with respect to annealing temperatures under varying atmospheres.

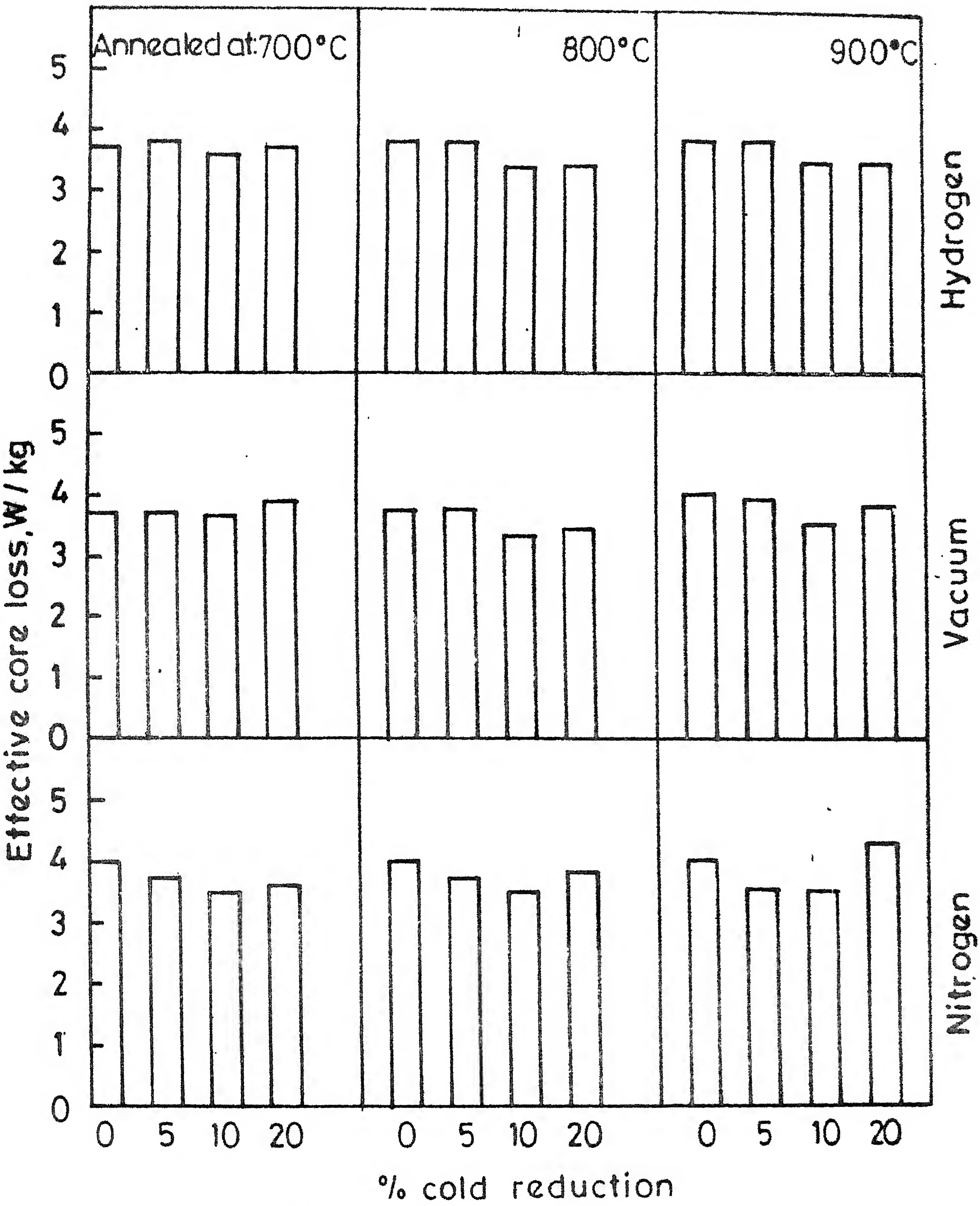

Fig. 3.10. Effective core loss of 300 grade silicon-steel cold worked and annealed in different atmospheres [redacted].

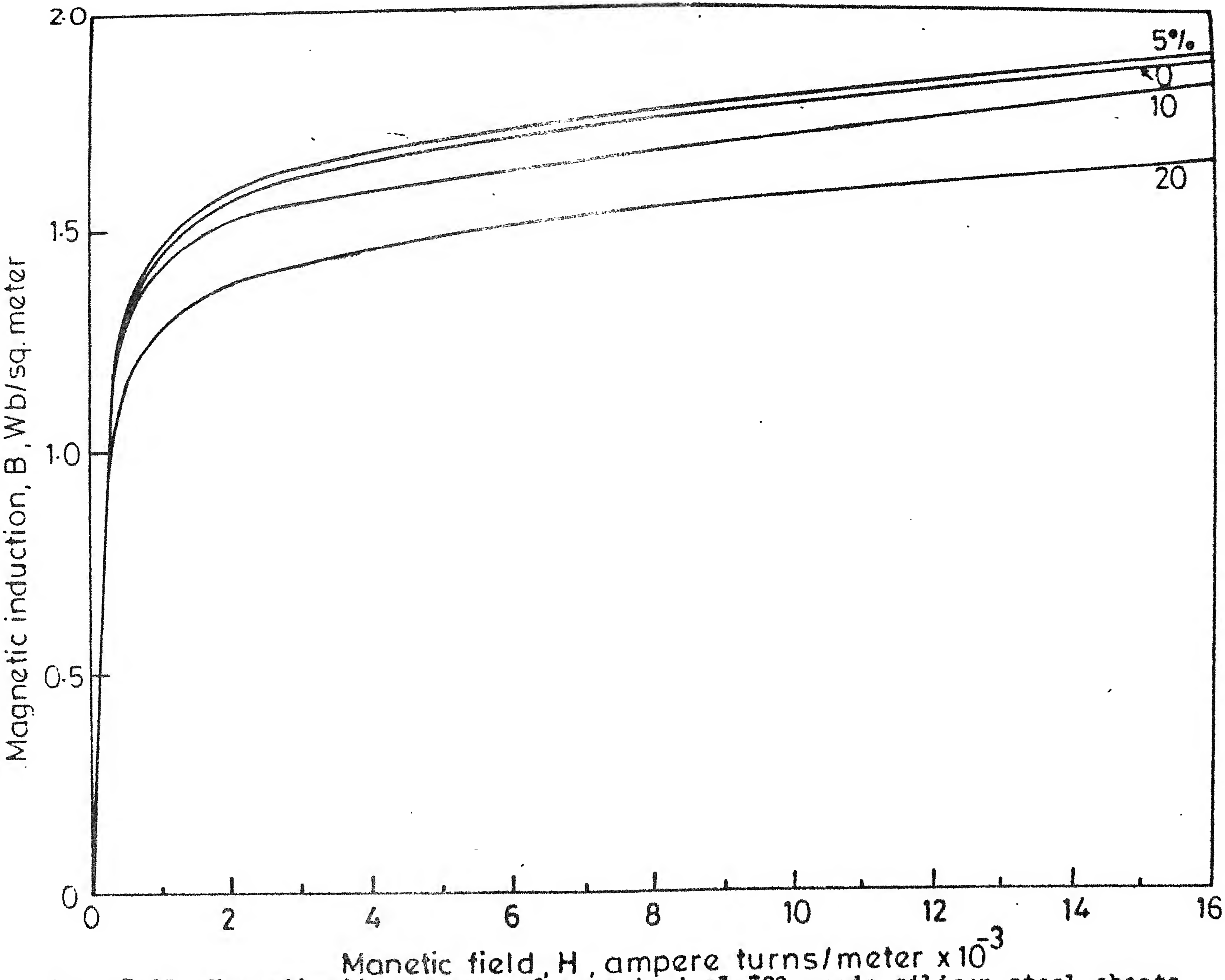

Fig. 3.11. Magnetization curves of some typical 300 grade silicon steel sheets cold-rolled to different levels and annealed at 800°C in hydrogen for 2 hours.

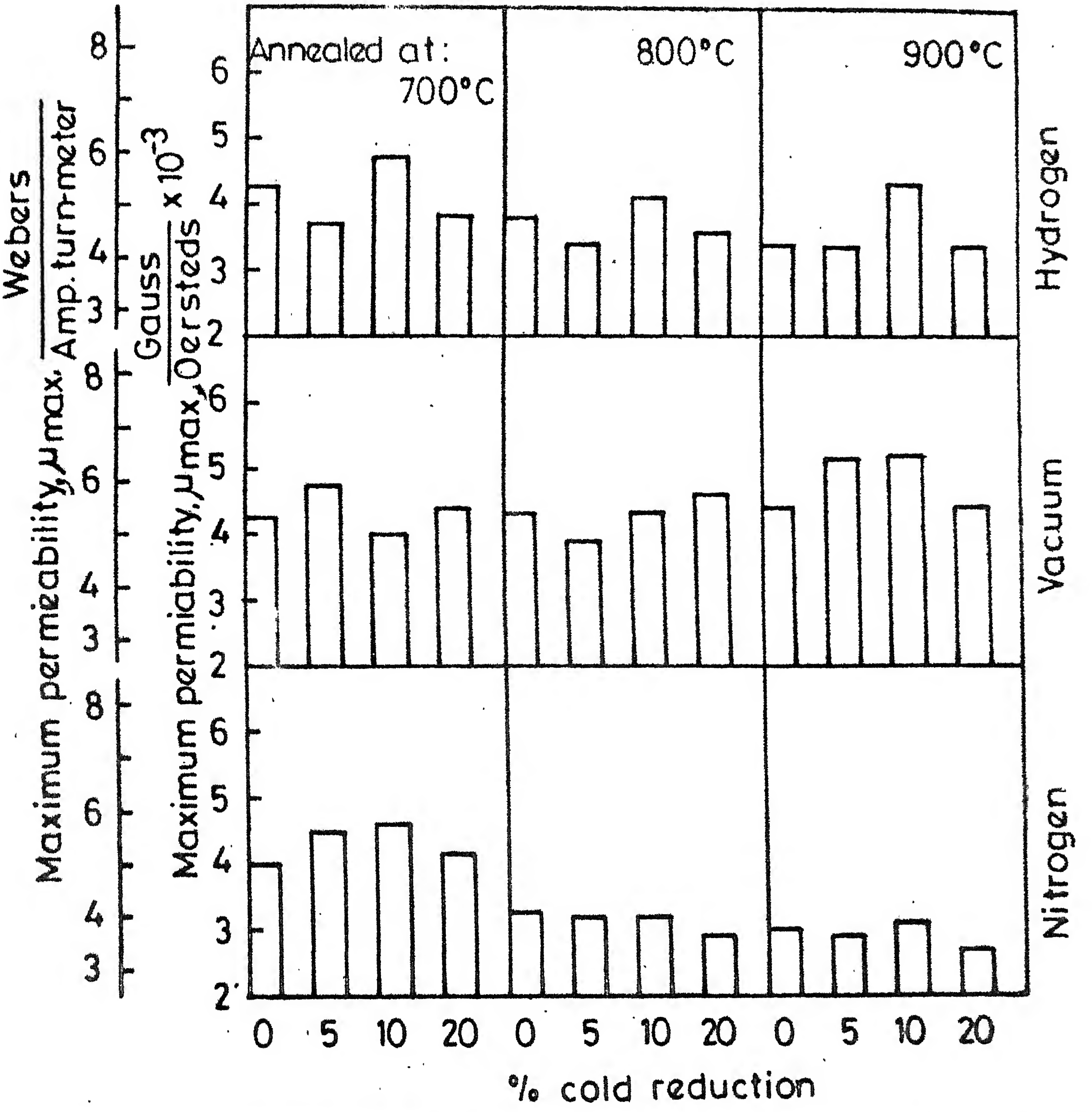

Fig. 3.12. Maximum permeability of 300 grade silicon-steel after varying cold-rolling and annealing treatments.

annealing temperatures and atmospheres. μ_{max} in nitrogen atmosphere is poorer than hydrogen or vacuum except in case of 700°C annealing, where the permeability is higher. At 700°C annealing the core-loss is more or less independent of annealing atmosphere, whereas the μ_{max} is highest in case of nitrogen annealing. Vacuum annealing gives best μ_{max} values at 800°C for samples cold-rolled to 0 pct. and 20 pct. respectively.

III.5.3 Magnetic Induction at 800 A/m:

Fig. 3.13 shows the magnetic induction at a magnetic field of 800 A/m (where the slope of the initial magnetization curve changes abruptly) for samples annealed in various atmospheres and at different temperatures. Magnetic induction at 800 A/m follows the same trend as in the case of maximum permeability plot (Fig. 3.12).

III.6 Brittleness

Fig. 3.14 shows the variation of brittleness of sheets in terms of number of reverse bends with annealing temperature and atmosphere for different levels of cold reduction. Results follow a similar trend as in the case of maximum permeability (μ_{max}). Lowest number of reverse bends is obtained in case of samples annealed in nitrogen atmosphere at 900°C.

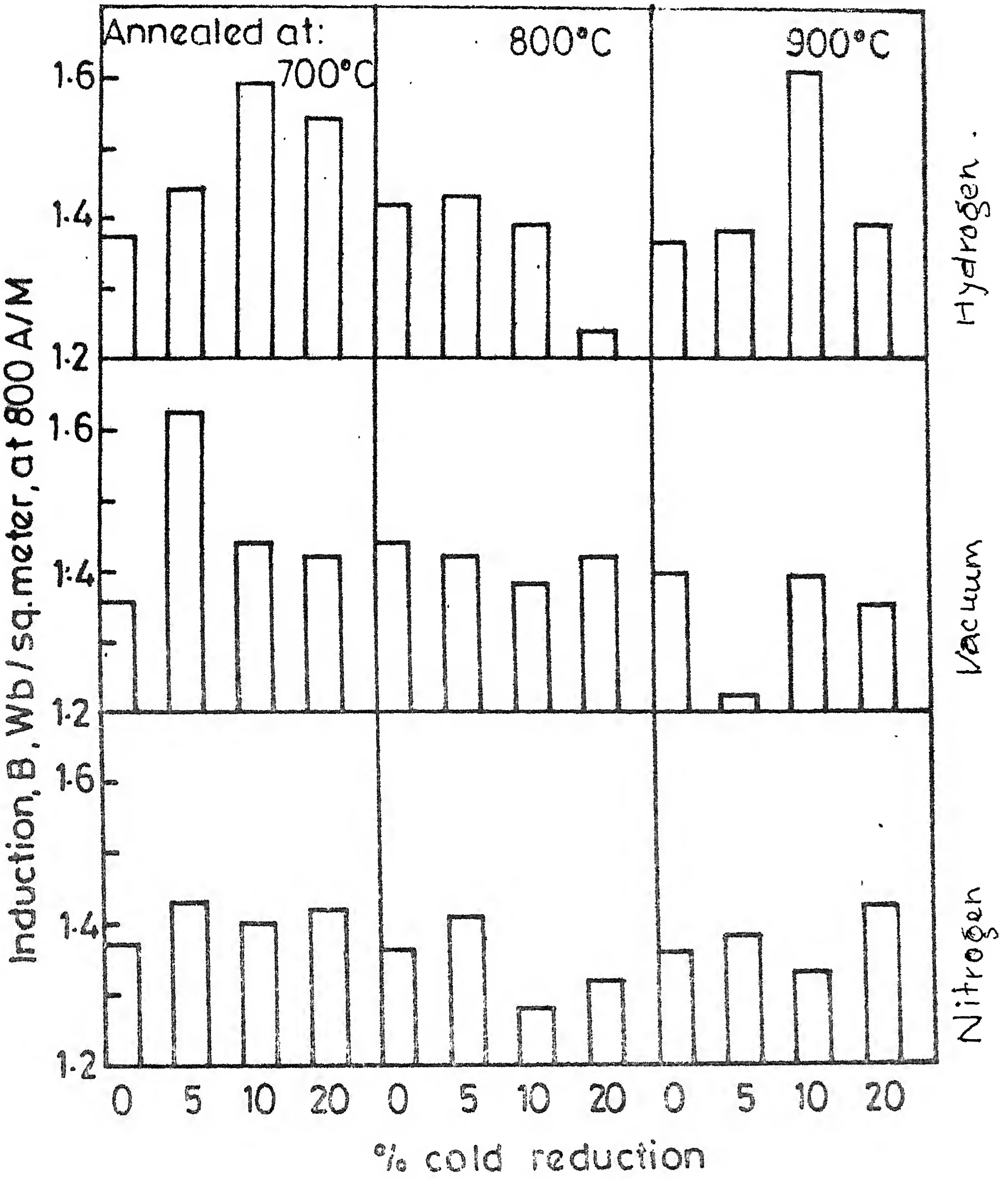

Fig. 3.13. Magnetic-Induction at 800 A/m magnetic field for 300 grade silicon-steel after varying cold-rolling and annealing treatments.

III.7 Chemical Analysis

Table 3.1 gives the chemical analysis of sheets annealed at various temperatures and atmospheres. Maximum decarburization is observed in case of vacuum annealing.

Table 3.1 Chemical analysis of silicon-steel sheets annealed at various temperatures and atmospheres

Atmosphere	Chemical analysis wt. pct.								
	700°C annealing			800°C annealing			900°C annealing		
	C	Si	S	C	Si	S	C	Si	S
Hydrogen	0.06	1.22	0.051	0.05	1.22	0.030	0.05	1.30	0.025
Nitrogen	0.08	-	0.024	0.08	0.940	.034	0.07	-	0.022
Vacuum	0.04	-	0.022	0.04	-	0.024	0.04	-	0.032

Part II

Chemically Coated and Annealed Silicon Steel-Sheets

III.8 Microstructure and Grain Size

Fig. 3.15 shows the microstructure of steels subjected to different chemical coatings and annealed at 900°C in hydrogen. The structure is ferrite with distinct grain boundaries.

Fig. 3.16 shows the variation of average grain size with annealing temperature and atmosphere for various coated sheet samples. The grain size is smallest in case of 900°C annealing except in the case of vacuum annealing. In the case of hydrogen annealing, the grain size is largest (120 μm) when annealed at 1000°C, but in case of vacuum and nitrogen atmosphere annealing such a feature is evidenced after 800°C annealing. The biggest grain size of (120 μm) is obtained in the case of coating no. 4 ($NaCl + MgO + KOH$), when annealed at 1000°C in hydrogen atmosphere. Annealing in nitrogen atmosphere results in smaller grains for any coated samples annealed at any temperature.

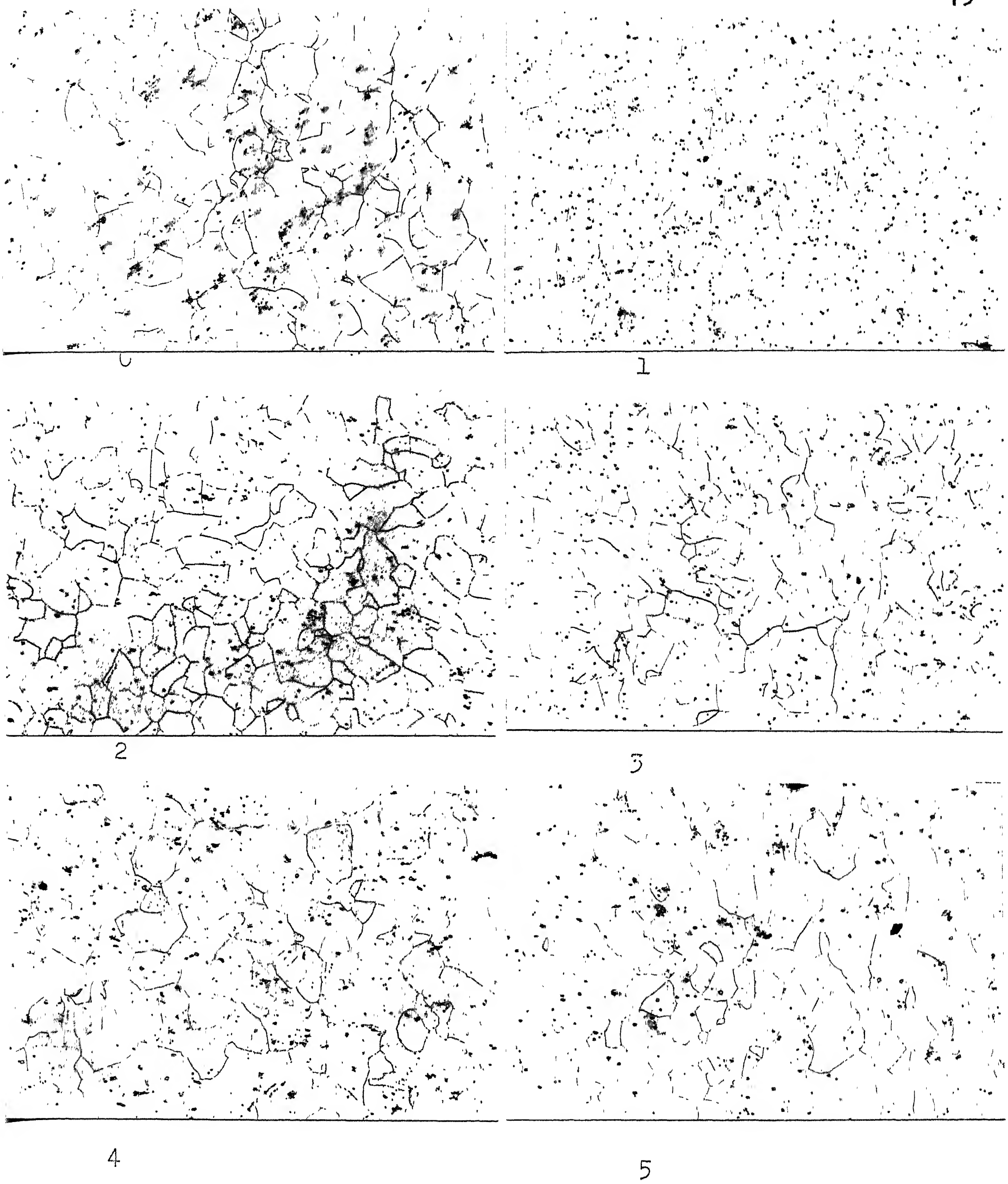

Fig. 3.15. Microstructures of 500 grade silicon-steel sheets annealed at 900°C after various chemical coatings (section parallel to the rolling plane) X 100.

0 - Uncoated, 1 - $MgCO_3$, 2 - $BaCO_3$ + MgO + KOH

3 - $CaCO_3$ + MgO + KOH, 4 - NaCl + MgO + KOH

5 - $Na_2CO_3.H_2O$ + MgO

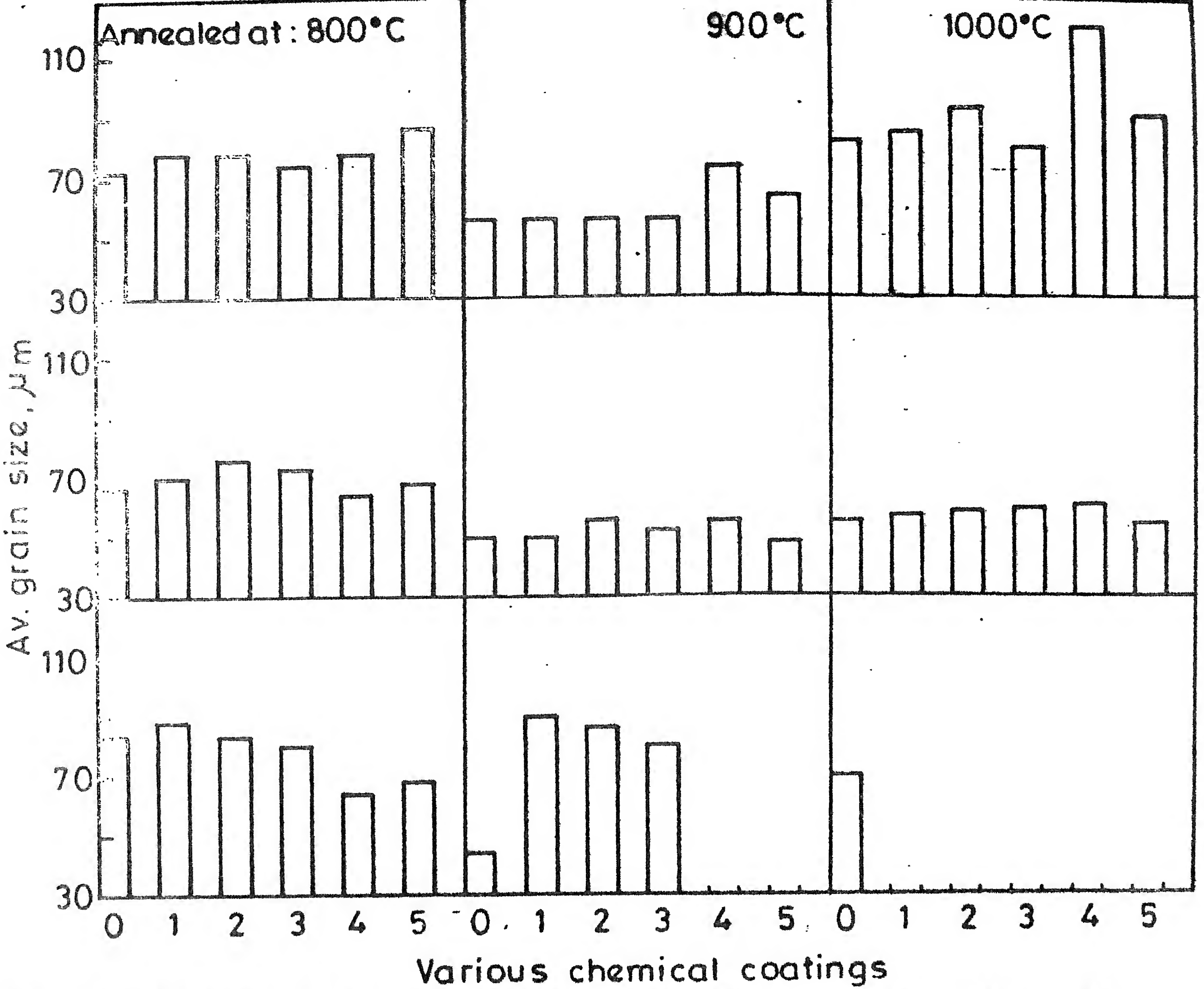

Fig. 3.16. Average grain size variation of chemically coated 300 grade silicon sheet along the hot-rolling plane after annealing in different atmospheres.
(Coating designations same as in Fig. 3.15).

III.9 Core-loss

Fig. 3.17 shows the core loss variation with annealing temperature and atmosphere for various coated samples. The lowest core loss is obtained after 900°C annealing in vacuum for coating no. 1 ($MgCO_3$). Coating no. 4 ($NaCl + MgO + KOH$), gives the lowest core loss after 1000°C annealing in hydrogen and nitrogen. Annealing at 1000°C in nitrogen results in highest core-loss for coating no. 3 ($CaCO_3 + MgO + KOH$). On the whole nitrogen annealing results in higher core-loss values of the sheets.

III.10 Initial Magnetization

Fig. 3.18 shows some typical initial magnetization curves (B-H) for coated samples annealed at 900°C in hydrogen atmosphere. It is apparent that there is not much change in the saturation magnetization for different coated samples.

III.10.1 Maximum Permeability (μ_{max})

Fig. 3.19 shows the maximum permeability (μ_{max}) variation of the coated silicon-steel annealed at different temperatures and atmospheres. The trend of variation of μ_{max} for different chemical coatings is similar for any annealing temperature or atmosphere.

III.9 Core-loss

Fig. 3.17 shows the core loss variation with annealing temperature and atmosphere for various coated samples. The lowest core loss is obtained after 900°C annealing in vacuum for coating no. 1 ($MgCO_3$). Coating no. 4 ($NaCl + MgO + KOH$), gives the lowest core loss after 1000°C annealing in hydrogen and nitrogen. Annealing at 1000°C in nitrogen results in highest core-loss for coating no. 3 ($CaCO_3 + MgO + KOH$). On the whole nitrogen annealing results in higher core-loss values of the sheets.

III.10 Initial Magnetization

Fig. 3.18 shows some typical initial magnetization curves (B-H) for coated samples annealed at 900°C in hydrogen atmosphere. It is apparent that there is not much change in the saturation magnetization for different coated samples.

III.10.1 Maximum Permeability (μ_{max})

Fig. 3.19 shows the maximum permeability (μ_{max}) variation of the coated silicon-steel annealed at different temperatures and atmospheres. The trend of variation of μ_{max} for different chemical coatings is similar for any annealing temperature or atmosphere.

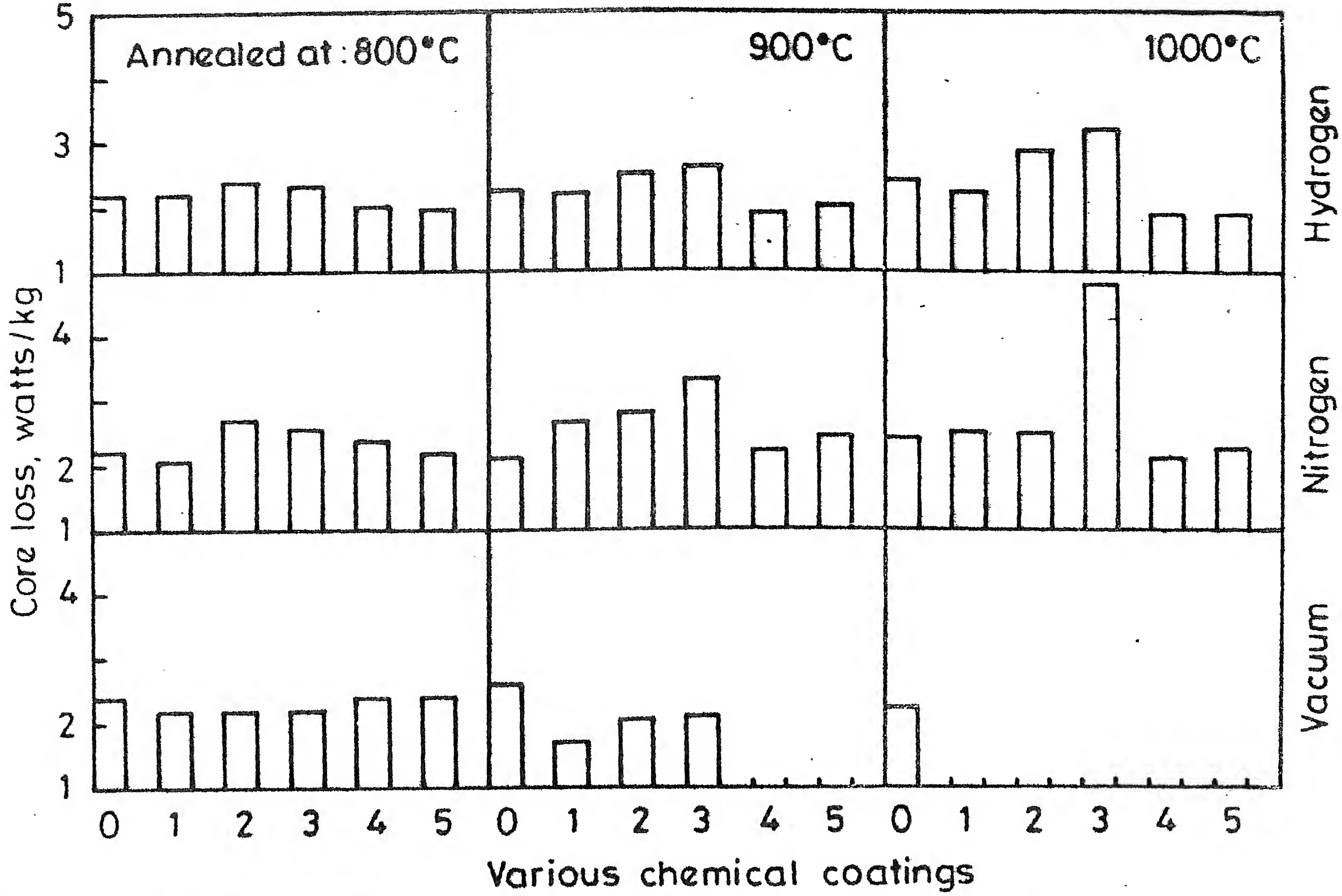

Fig. 3.17. Core-loss variation of chemically coated 300 grade silicon steel sheets after annealing in different atmospheres. (Coating designations same as in Fig. 3.15).

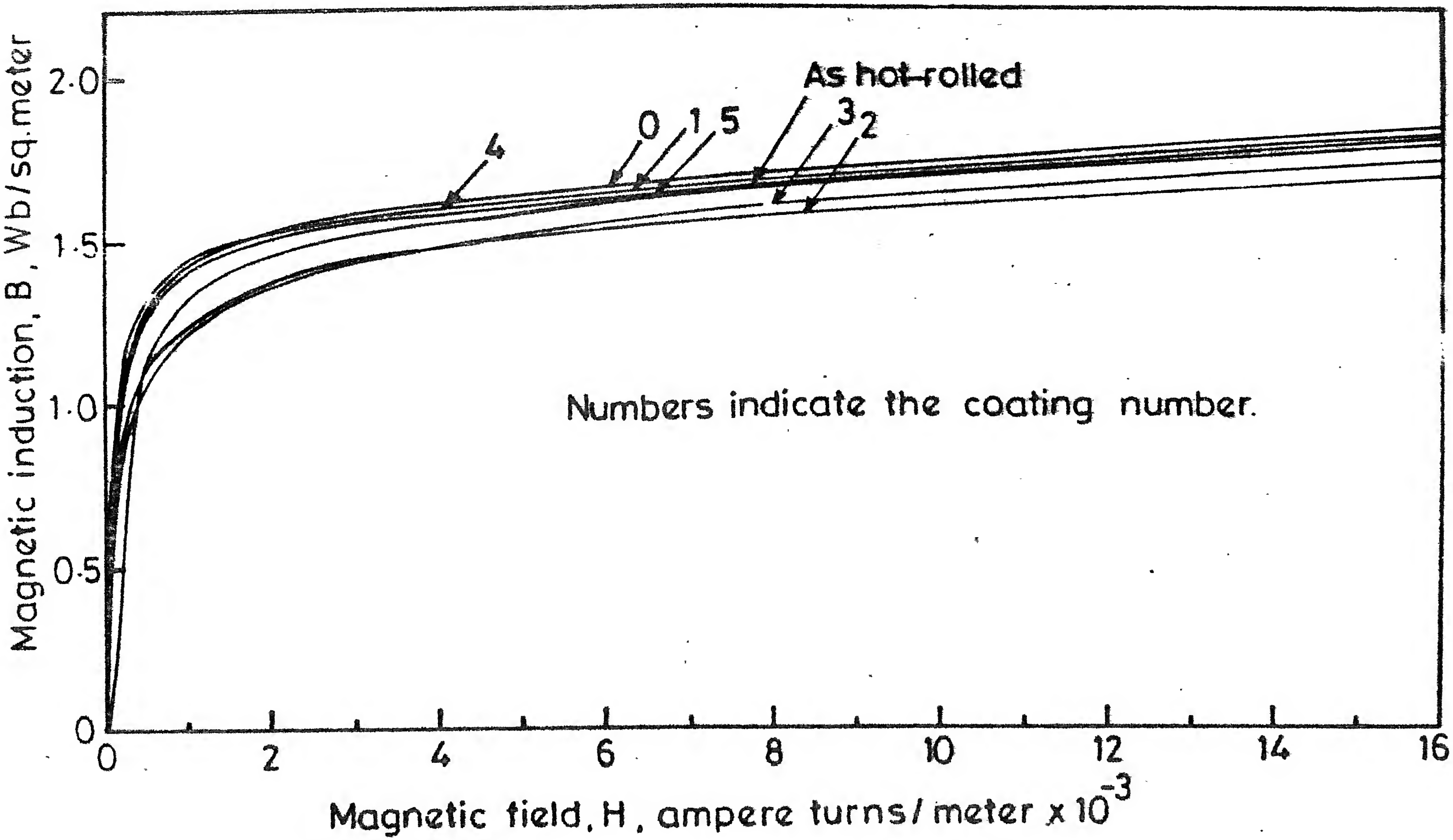

Fig. 3.18. Magnetization curve band of 300 grade silicon-steel sheets chemically coated and annealed in hydrogen at 900°C for 2 hours, (Coating designations same as in Fig. 3.15).

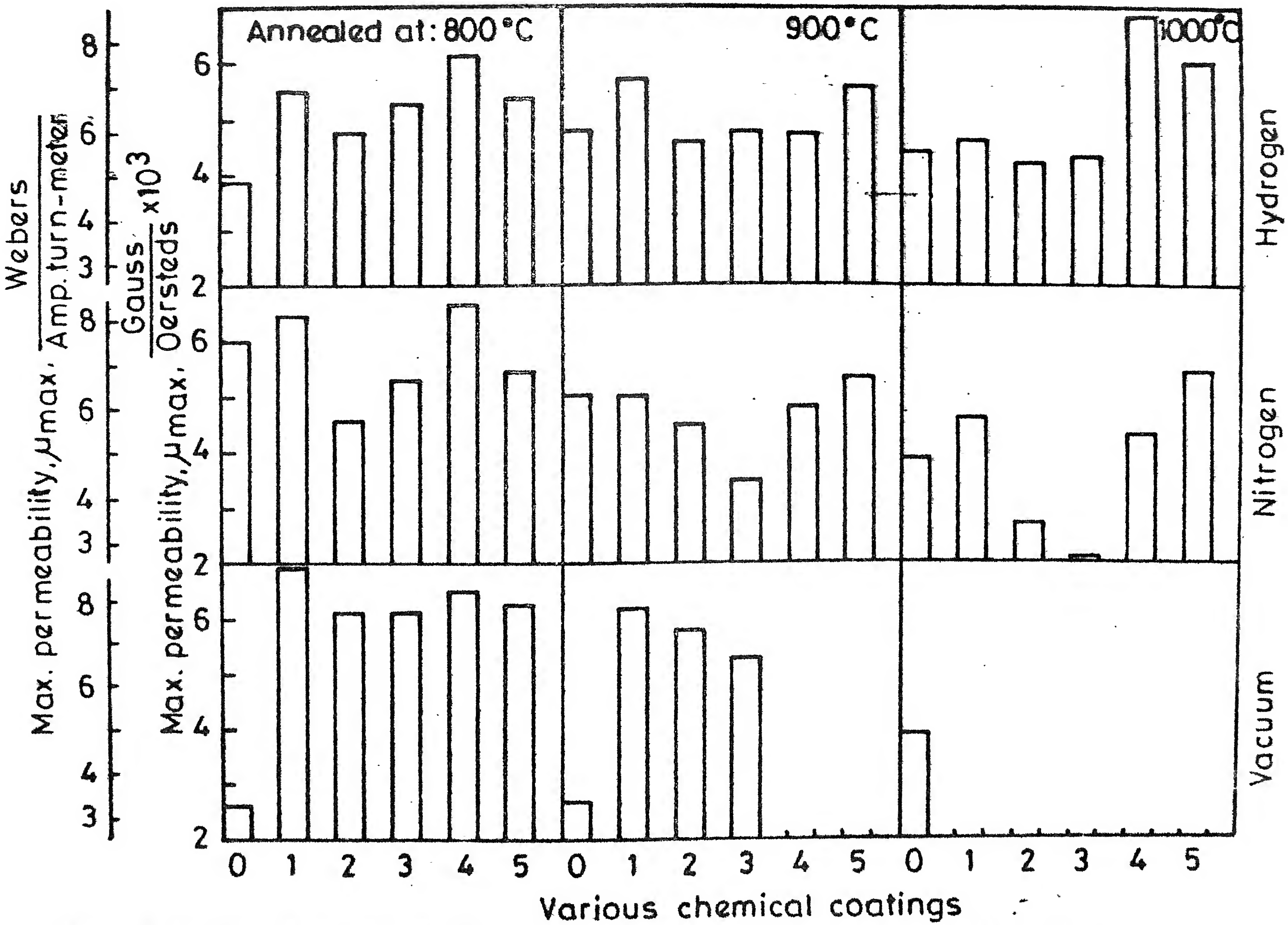

Fig. 3.19. Maximum permeability of 300 grade silicon steel sheets after different chemical coating and annealing in various atmospheres.
(Coating designations same as in Fig. 3.15).

III.10.2 Induction at 800 A/m Field

Fig. 3.20 shows the magnetic induction (at 800 A/m field) variation of the coated samples annealed at different temperatures and in various atmospheres. The trend is similar as in the case of maximum permeability (μ_{max}) variation (Fig. 3.19).

III.11 Brittleness

Fig. 3.21 shows the brittleness variation (in terms of number of reverse bends) of the coated samples for various annealing temperatures and atmospheres. It is apparent that annealing in hydrogen atmosphere gives the best reverse bend values.

III.12 Chemical Analysis

Table 3.2 gives the chemical analysis of the coated silicon-steel samples after annealing in various atmospheres at 900°C. The lowest level of carbon (0.03 pct.) is achieved for coating no. 5 ($Na_2CO_3 \cdot H_2O$ + MgO) when annealed in nitrogen atmosphere. Maximum desulphurization is obtained in case coating no. 3 ($CaCO_3$ + MgO + KOH), when steel is annealed in hydrogen.

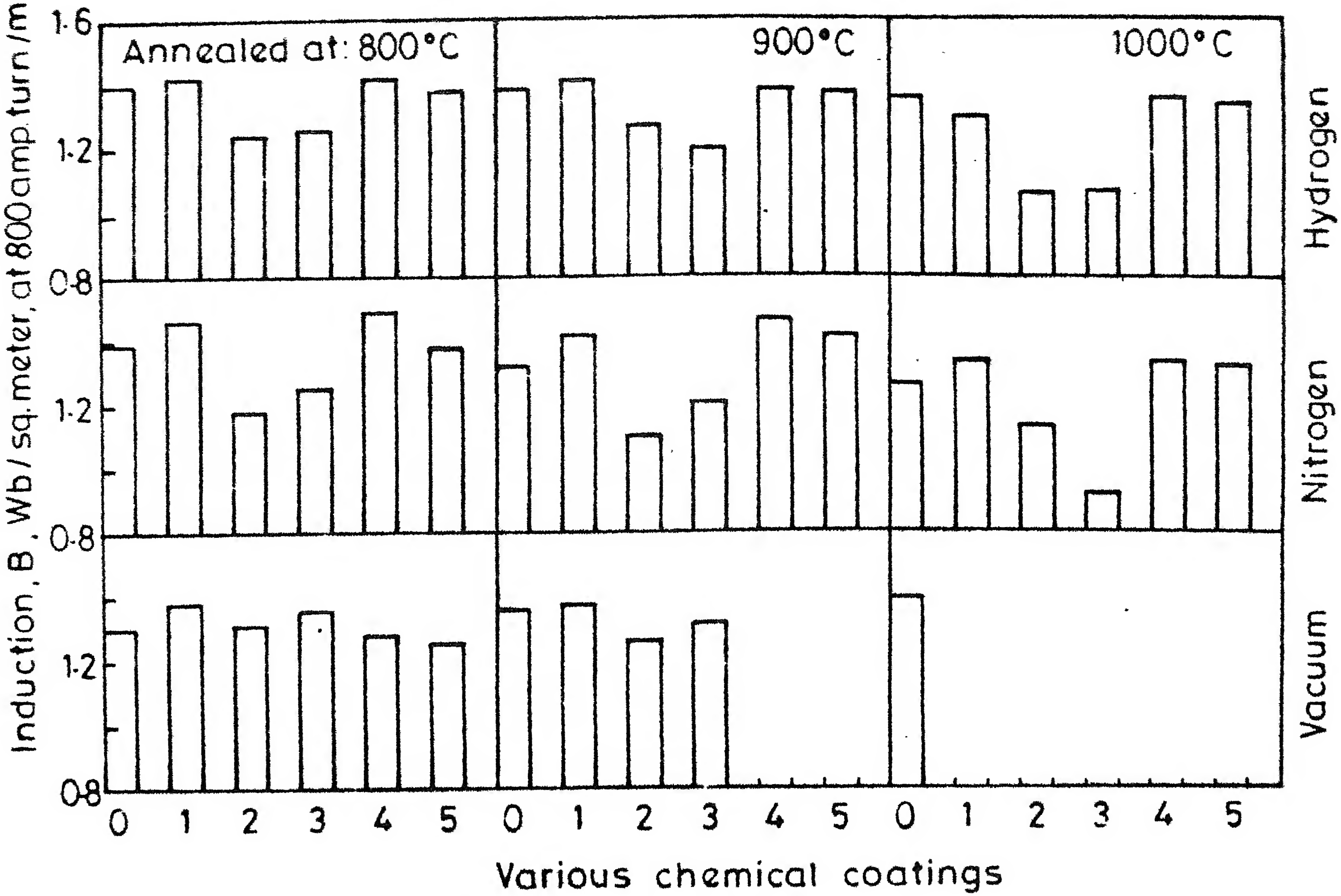

Fig. 3.20. Magnetic Induction at 800 A/m magnetic field for 30 grade silicon steel after different chemical coating and annealing in various atmospheres.
(Coating designations same as in Fig. 3.15).

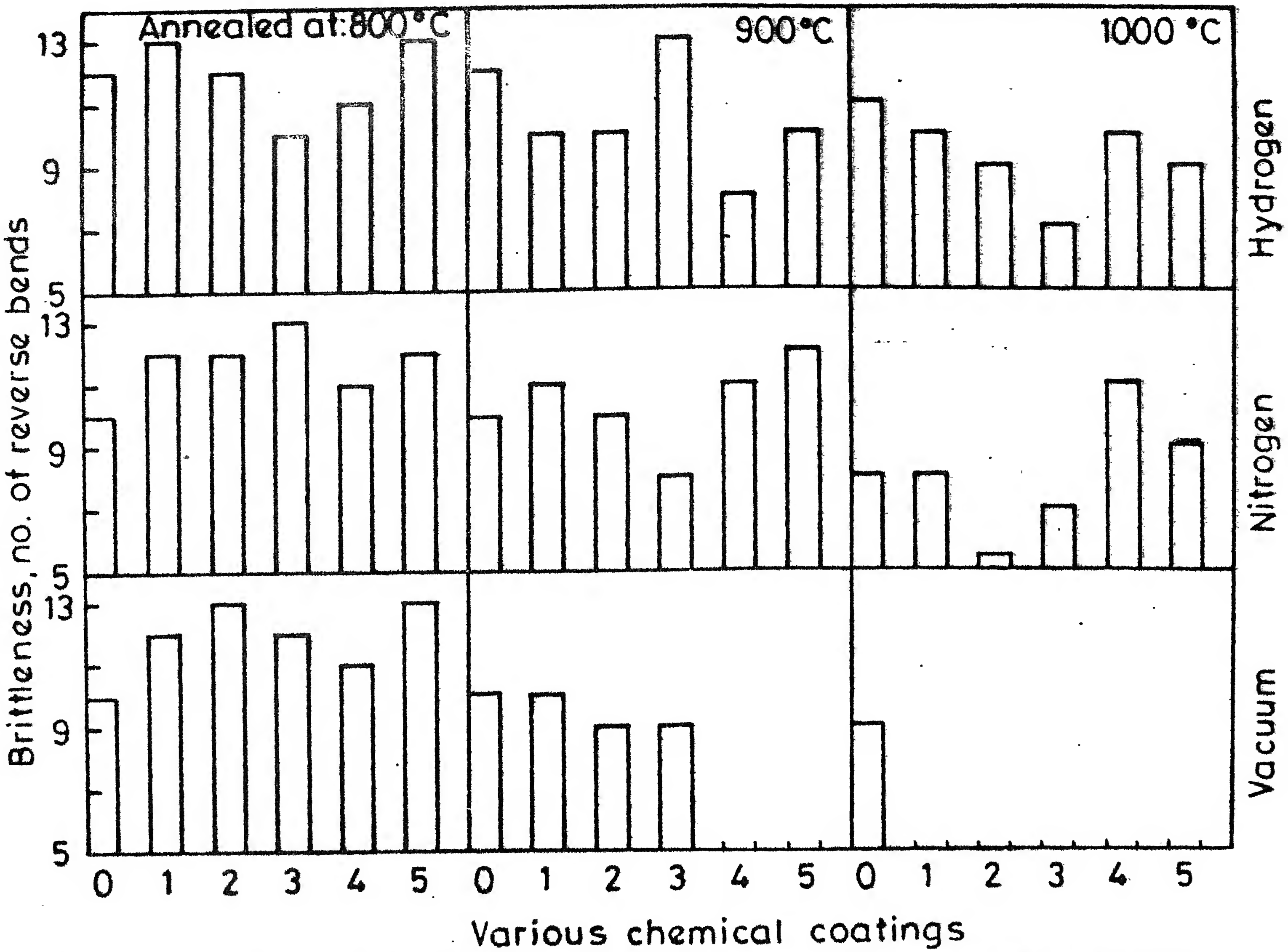

Fig. 3.21. Brittleness of chemically coated silicon-steel sheets after various annealing treatments (0.50 mm thick). (Coating designations same as in Fig. 3.15).

Table III.2 Chemical analysis of coated silicon steels after annealing at 900°C in various atmospheres.

Annealing atmosphere	element	Various chemical coatings					
		0	1	2	3	4	5
	C	0.05	0.05	0.08	0.07	0.05	0.04
Hydrogen	S	0.03	0.031	0.02	0.018	0.024	0.024
	Si	1.24	1.24	1.22	1.22	1.31	1.31
	C	0.04	0.04	0.05	0.05	0.07	0.03
Nitrogen	S	0.02	0.027	0.026	0.022	0.027	0.020
	Si	1.03	1.35	1.50	1.41	1.41	1.31
	C	0.08	0.05	0.040	0.04	-	-
Vacuum	S	0.03	0.03	0.027	0.030	-	-
	Si	1.27	1.31	1.31	1.31	-	-

CHAPTER IV

DISCUSSION

There are two ways by which the electrical properties of silicon steel sheet can be improved. These are either by change in the steel composition or by change in the grain size by various finishing treatments of the sheet. For the same silicon level in steel, further improvement in the quality is possible if very low levels of residual impurities like carbon, sulphur, phosphorus and manganese etc. are achieved during steel making. For a conventional steel making process it is rather difficult and uneconomical to produce steels with very low levels of impurities.

It is a well known fact that for any composition, with increase in the grain size, the electrical losses in the silicon-steel decrease. Further, through the application of recrystallization and grain-growth, optimum grain size of the steel can be achieved. Additional improvements in the quality can be achieved when processes like de-carburization, de-sulphurization, de-oxidation etc. result during the annealing treatment. Different chemically active coatings have also been tried for this purpose in the past [30].

The present investigation has been aimed at an improvement in the electrical and magnetic properties of the hot-rolled dynamo-grade silicon steel sheets entirely through the finishing treatments. For this, various cold-reductions followed by annealing and the use of chemically active coatings which might effect decarburization and desulphurization during annealing of the sheets have been discussed under two separate parts.

Part - I

Effect of Annealing on Grain Size Control

IV.1 Recrystallization and Grain-Growth

It has been earlier established[21,22] that the application of a critical cold-reduction for any silicon-steels results in the largest grain size. The present investigation reveals that the grain size is maximum at a critical cold-reduction of 10 pct., after annealing at any temperature in any atmosphere (Fig. 3.6). The microstructure of as received hot-rolled sheet (Fig. 3.1) reveals the fact that the structure is not a completely recrystallized one. This was probably due to the low-finishing temperature or heavier reduction in the last pass during hot-rolling. Thus, even without any cold reduction, few recrystallized grains

appear after annealing, but its rate is significantly low. Most of the internal strains are relieved during annealing through change in the grain shape. At relatively low cold reduction, i.e. say 5 pct., only a few grains recrystallize which grow at the expense of the neighbouring strained-grains. Thus the average grain size after annealing practically remains unchanged. However, at a critical cold reduction of 10 pct., optimum number of nucleated grains grow consuming most of the strained grains. With further increase in cold-reduction viz. 20 pct., many more number of nucleated grains appear which grow at the same time such that the resultant grain size after annealing is rather small.

It appears that the grain growth variation in the present case is faster with the increase in annealing temperature. Further, the grain size achieved presently in case of 800°C is larger than that of 700°C annealing. But, when the annealing temperature was further increased, faster grain nucleation appears to occur due to the availability of higher thermal energy. This results in many grains growing at the same time, thus giving rise to a fine grain size. This confirms with the trend reported by several workers[19,20].

As far as the effect of annealing atmosphere is concerned, the overall grain coarsening is maximum in case of

vacuum annealing as compared to other annealing atmosphere, such as hydrogen or nitrogen. This is due to the fact that vacuum resulted in the maximum decarburization of the steel. Grainsize obtained in case of hydrogen annealing is larger than in the case of nitrogen annealing. This is probably due to the higher extent of decarburization through the following reaction in the case of hydrogen annealing (Table III.1).

$$C + 2H_2 = CH_4, \quad G^{o}_{1000^{o}K} = -7640 \text{ cals}$$

With the prevailing conditions, this reaction proceeds in the forward direction and the rate is faster when the temperature is high. Thus, it is evident that the change in grain size combined with decarburization affect the core loss property.

The magnitudes of grain size of the sheets cold worked along the parallel or perpendicular direction to the hot rolling direction are approximately similar. This confirms with the literature[28], which reports that grain growth after recrystallization is independent of the direction of cold-rolling of the sheets.

The aspect-ratio of grains increases with the extent of cold-reduction (Fig. 3.8). This is obvious, as higher the extent of cold-reduction, the anisotropy induced is higher in

the direction of cold-rolling. When the cold-rolling was done in a perpendicular direction to the hot-rolling, the aspect ratio tends to a value of unity due to the fact that elongated grains after hot-rolling (Fig. 3.1) get flattend due to rolling in the perpendicular direction. The results that the grain aspect ratio for any level of cold-reduction increases in the order 900°C → 800°C → 700°C for any annealing atmosphere excepting vacuum, can be explained on the basis that the increase in annealing temperature the number of growing orientation free grains (equiaxed) increases and the directionality of grains is lost.

IV.2 Electrical and Magnetic Properties

IV.2.1 Core-loss

The electrical losses for the Si-steel measured presently decrease with increase in grain size. This is an established feature[10,18,19] that with the increase in grain size, the loss due to hysteresis decreases, whereas the eddy-current loss increases. Thus there is an optimum grain size for which the coreloss is minimum. The trend in the variation of the core loss values (Fig. 3.9 and Fig. 3.10) confirms with that obtained with the grain-size plots (Fig. 3.6 and Fig. 3.7). This confirms that the improvement

in the electrical property, i.e.,decrease in core loss is purely attributed to the increase in grain size after the critical cold reduction.

IV.2.2 Initial Magnetization

The saturation magnetization characteristic of 300-grade silicon-steel is virtually unaffected (Fig. 3.11) at low levels of cold-reduction, but, when the cold-reduction increases (in this case upto 20 pct.), induction decreases.

The maximum permeability (μ_{max}) of any magnetic steel is a structure sensitive property[4]. With increase in annealing temperature, the maximum permeability has a decreasing tendency (Fig. 3.12) in case of hydrogen or nitrogen annealing, though this trend is absent in case of vacuum annealing. With increase in annealing temperature, the degree of grain-orientation due to prior cold work is lost which decreases the maximum permeability values. A further decrease in 'μ_{max}' values in the case of nitrogen annealing results due to probably nitrogen diffusion into the steel.

IV.3. Brittleness

It is desired that the brittleness of the silicon-steel sheets should be low, as higher brittleness causes

difficulty in handling and punching operations. In commercial practice, this brittleness is measured in terms of number of reverse bends the sheet can take till the appearence of fracture. The results of the present investigation reveal that brittleness (Fig. 3.14) increases with the increase in annealing temperature, particularly in case of nitrogen annealing. With increasing cold-reduction and temperature of annealing the possibility of enhanced nitrogen diffusion into the steel is more which may embrittle the material. Similar types of correlation have been observed in the case of μ_{max} plots also.

IV.4 Effect of Annealing Atmosphere on Steel Composition

Table III.1 reveals that the effect of vacuum or hydrogen annealing on steel composition is more than in nitrogen annealing. This can be explained on the basis that during vacuum annealing, the carbon in the steel diffuses out and combines with the oxygen in the scale, if any, while in the case of hydrogen annealing, hydrogen reacts with the carbon on the surface of the sheet to form CH_4 and hence better decarburization.

Part II

Effect of Chemical Coatings

The purpose of giving the chemical coatings prior to annealing on to the sheet surface is to improve the electrical and magnetic properties of the 300 grade silicon steel sheets through decarburization, and desulphurization. Accordingly the various chemical compounds were selected. These coatings have been tried and reported elsewhere[30] for improving the quality of transformer grade sheets. It was assumed that the dynamo-grade sheets can also be improved by the employment of the same principles. Further, it has been reported that the presence of NaCl and Na_2CO_3 as coating components favours desulphurization of the steel[30].

To economise the total annealing time, samples coated with various carbonates such as $CaCO_3$, $MgCO_3$ and $BaCO_3$ (Table II.1) were annealed together. Similarly samples coated with different alkaline compounds like $Na_2CO_3.H_2O$ and NaCl were annealed together. Coatings in the first group (carbonates) when heated decompose into their respective oxides and carbon dioxide gas. The carbon dioxide is expected to act as the decarburizing agent for the sheets. The decaburization reaction of '$\underline{C} + CO_2 = 2CO$' occurs on the

surface of the sheet at the metal/coating interface. The rate of this decarburization reaction is controlled by the diffusion of carbon along the sheet thickness and the $\frac{p_{CO}}{p_{CO_2}}$ ratio. As the samples coated with different coatings were annealed together, the different reactions involved are rather complicated and it is very difficult to find out the effect of each individual coating quantitatively. Therefore the effects of the various coatings are analysed qualitatively and the performance of any coating in particular is evaluated from its effect on the electrical and magnetic property.

KOH was used to get an alkaline medium which eliminates the rusty spots and the staining of the coated samples. This also makes the coating more uniform and adherent [30]. In case of coating no. 1 ($MgCO_3$), it resulted in staining and rusty spots after the samples are coated, whereas this was not observed in the case of other coatings (Table II.2).

In all the coatings MgO was one of the components including coating no. 1 ($MgCO_3$), where it was obtained after decomposition at the respective annealing temperatures. MgO reacts with SiO_2 in the steel forming '$MgSiO_3$' according to the following reaction within a temperature ranging from room temperature to 1327°C [36].

$$MgO + SiO_2 = MgSiO_3, \quad G^{o}_{1173^{o}K} = -7609.7 \text{ Kcal}$$

$MgSiO_3$ thus formed on the surface of the sheets acts as an insulating layer which decreases the eddy current loss[4].

All the carbonates used as coating components viz. $MgCO_3$, $BaCO_3$ and $CaCO_3$, decompose when heated to the annealing temperatures. The various decomposition reactions concerned are as follows[36].

$MgCO_3 = MgO + CO_2$ (decomposition temp. 350-900°C)

$BaCO_3 = BaO + CO_2$ (decomposition temp. 806-958°C)

$CaCO_3 = CaO + CO_2$ (decomposes at all temperatures)

The CO_2 generated reacts with the carbon in the sheet surface and results in decarburization, according to the following equation.

$$\underline{C} + CO_2 \rightleftharpoons 2CO$$

This is a reversible reaction and is mostly dependent on temperature and $\frac{CO}{CO_2}$ ratio. With the conditions prevailing in the present investigation, the above reaction proceeds in the forward direction. The rate of carbon removal is dependent mainly on the quantity of the CO_2 generated from the coating and the prevailing temperature. Further, the rate of decarburization is also dependent on the diffusivity of carbon atoms in the steel at any particular temperature.

The quantity of CO_2 generated from each type of coating under present set of experiments was calculated and found to decrease in the order $MgCO_3 \rightarrow CaCO_3 \rightarrow BaCO_3$, the ratio being 3:2.1. It is therefore expected that $MgCO_3$ would result in the highest degree of decarburization, when other factors are unchanged. Therefore, maximum improvement in core loss property is obtained in case of $MgCO_3$ coating when subjected to vacuum annealing.

IV.5 Grain Size

The change in grain size of the coated samples (Fig. 3.16) is mostly due to the variation of annealing temperature which controls the recrystallization characteristics. The microstructure of as received hot rolled sheet (Fig. 3.1) reveals that the recrystallization during hot rolling was incomplete. It is rather difficult to identify the exact parameters in case of different samples which affect the grain size other than that discussed above.

IV.6 Electrical and Magnetic Properties

As the present investigation reveals that the type of coating under a set condition of annealing is not sensitive in imparting any appreciable change in the grain size of the steel, the difference in the core-loss is thus mostly due to

factors other than grain size, i.e., decarburization, desulphurization etc. Although it is difficult to quantify the effects of such processes on the core-loss property, a qualititative approach is worth mentioning. As already indicated in earlier section, the coating yielding maximum CO_2 gas should result in the highest degree of decarburization. This is confirmed from the core-loss plot (Fig. 3.17). For example, in case of samples coated with 'K_2CO_3', minimum core-loss after annealing in vacuum was observed coating No. 4 (NaCl + MgO + KOH) and No. 5 (Na_2CO_3 + MgO) have resulted in comparatively lower core-losses after annealing. This is possibly due to some degree of desulphurization[30] which is confirmed from the chemical analysis (Table III.2) of some typical specimens.

With the increasing magnetic softness of the steel, i.e., when the core-loss decreases, the maximum permeability increases. The maximum permeability plot (Fig. 3.19) shows a similar trend as obtained in the case of core-loss. Coating nos. 2 and 3 give higher core-loss values and correspondingly the maximum permeabilities are lower. On the other hand in case of samples coated with coating no. 1, 4 or 5, lower core-loss values are obtained as compared with samples coated with coating nos. 2 or 3 and the maximum permeability in this case is higher. This trend is true for almost all the temperatures and atmospheres of annealing.

IV.7. Brittleness

With the increase in the annealing temperature, the grain coarsening increases. Therefore the brittleness plot (Fig. 3.21) shows a gradual decrease in reverse bend values with increase in the annealing temperature. In case of nitrogen annealing the lowest number of reverse bends obtained which is possibly due to nitrogen pick-up as explained in the case of cold-rolled sheets.

CHAPTER V

CONCLUSIONS

1. It is always possible to improve on the electrical and magnetic properties of hot-rolled, dynamograde silicon-steel sheets through different finishing treatments viz critical cold-reduction and the use of chemically active coatings to facilitate decarburization and desulpharization processes.

2. For a 300-grade steel-sheet containing 1.42 pct. silicon, the critical cold reduction which results in the largest grain size after annealing is about 10 pct.

3. Annealing of the cold-rolled silicon-steel sheets at 800°C results in the largest grain size. On further increase in the annealing temperature grain size becomes finer.

4. The core losses corresponding to the critical level of cold-reduction of 10 pct. and annealing temperature of 800°C are minimum. The maximum permeability, μ_{max}, values after various annealing treatments are maximum corresponding to the minimum core loss values.

5. Samples coated with $MgCO_3$, NaCl and Na_2CO_3 improves the electrical and magnetic properties of the dynamo grade silicon-steel after annealing whereas coatings containing $BaCO_3$ and $CaCO_3$ deteriorate the properties.

6. Brittleness of the annealed, 300-grade sheets is a function of atmosphere, such as it is lowest in case of hydrogen annealing, but is not a function of annealing temperature, where it remains more or less constant. The chemical coatingsdo not appear to have much influence on the brittleness.

7. In general vacuum annealing results in the best electrical properties followed by hydrogen and nitrogen.

BIBLIOGRAPHY

1. Satoru TAGUCHI,
Trans. I.S.I. Japan, 17, 1977, 604.

2. K.L. Narasaya, M.D. Maheswari, U.K. Jha, T. Mukherjee,
Trans. Indian Inst. of Metals, 33, 1980, 139.

3. R.V. Tamhanker,
TISCO Technical Journal, 3, 1956, 95.

4. R.M. Bozorth, 'Ferromagnetism'.
D. Van Nostrand Company, Inc., New York, 1964.

5. T. Spooner, 'Properties and Testing of Magnetic Materials',
McGraw-Hill Book Company, Inc., New York, 1927.

6. G.N. Shubin, V.V. Druzhinin, V.A. Koroleva,
Stal in English, 5, 1961, 358.

7. M. Stankiewicz,
HUTNIK 24, 1957, 266 (H.B. Translation No. 4153).

8. Y.D. Yensen,
Stabl-und-Eisen, 56, 1936, 1545.

9. T.D. Yensen,
Trans. American Inst. of Elect. Engineers, 33, 1914, 451.

10. T.D. Yensen,
Trans. American Inst. of Elect. Engineers, 43, 1924, 145.

11. G.A. Garnyk and A.M. Samarin,
'Primenenie Vakuuma V metallurgii, Moscow, 1958.
(Translations from a collection of papers, entitled use of vacuum in metallurgy, H.B. Translation No. 4362).

12. A.M. Samarin, L.M. Nomvik,
Stal, 16, 1956, 700.

13. N.F. Dubrov,
Stal, 18, 1958, 246.

14. A. Pomp and H. Wubbenhorst,
Stahl und Eisen, 62, 1942, 482 (H.B. Translation No. 1361)

15. A.G. Pietrienko,
HUTNIK, 24, 1957, 277 (H.B. Translation No. 4145).

16. M.I. Kolov, L.P. Ershova and N.M. Selivanov,
Stal, 22, 1962, 637.

17. S. Mishra and V. Ramaswamy,
Trans. Indian Inst. of Metals, 32, 1979, 20.

18. W.E. Ruder,
Trans. American Society of Metals, 22, 1934, 1132.

19. Research Report No. 34/45, Tata Iron and Steel Co.
Ltd., Jamshedpur.

20. A. Wimmer and P. Werthebach,
Stahl und Eisen, 54, 1934, 385 (H.B. Translation No. 22).

21. B.F. Trakhtenberg,
Stal, 16, 1956, 343 (H.B. Translation No. 3838).

22. B.G. Livshits, B.I. Mindlin, et.al.
Fiz. metal metalloved, 40, 1975, 163.

23. P. Cotterill and P.R. Mould, 'Recrystallization and
grain growth in metals',
Surrey Univ. Press., London, 1976.

24. 'Progress in Metal Physics, Vol. 3', Bruce Chalmers (Ed.), Pergamon Press, London, 1952.

25. R.E. Reed-Hill, 'Physical Metallurgy Principles', D. Van Nostrand Company, New York, 1958.

26. C.G. Dunn and J.L. Walter, 'Recrystallization, grain growth and Textures in Metals'.
ASM, Metals Park, Ohio, 1966.

27. Koh MATSUMURA, Akio KAMADA,
Trans. I.S.I. Japan, 13, 1973, 174.

28. Hitoshi Nakae and Kohsuke Tagashira,
Trans. Japan Inst. of Metals, 14, 1973, 15.

29. V.G. Paranjpe,
TISCO Technical Journal, 1, 1954, 115.

30. N.I. Lapkin,
Fizika Metallovi Metallovedenie, 1, 1955, 155.
(H.B. Translation No. 3628).

31. T.D. Yenson,
Stahl und Eisen, 52, 1936, 1548.

32. H.H. Meyer and H. Schlutter,
Stahl und Eisen, 73, 1953, 1706.

33. L. Birks, 'Conference on Decarburization',
I.S.I. Publication No. 133, 1970.

34. K.V. Dnepronko and V.G. Borisenko,
Stal in English, 22, 1962, 719.

35. Private Communication with A.M. Gokhle,
Indian Institute of Technology, Kanpur.

36. O. Kubaschowski and C.B. Alcock,
'Metallurgical Thermochemistry',
Pergamon Press, Oxford, 1979.